Journal of Hazardous Materials 458 (2023) 131940

Contents lists available at ScienceDirect

Journal of Hazardous Materials

journal homepage: www.elsevier.com/locate/jhazmat

Research Paper

Impact of compacted bentonite microbial community on the clay mineralogy and copper canister corrosion: a multidisciplinary approach in view of a safe Deep Geological Repository of nuclear wastes

Marcos F. Martinez-Moreno [a,*], Cristina Povedano-Priego [a], Mar Morales-Hidalgo [a], Adam D. Mumford [b], Jesus J. Ojeda [b], Fadwa Jroundi [a], Mohamed L. Merroun [a]

[a] Department of Microbiology, Faculty of Sciences, University of Granada, Granada, Spain
[b] Department of Chemical Engineering, Faculty of Science and Engineering, Swansea University, Swansea, United Kingdom

HIGHLIGHTS

- No evidence of illitization of smectite in the highly-compacted bentonite was observed over one year.
- Increase of aerobic bacteria belonging to Micrococcaceae and *Nocardioides* in heat-shock bentonites was detected.
- Sulfate-reducing bacteria exhibited survival after one year incubation under anoxic, dry and heat shock conditions.
- The growth of SRB was stimulated by the presence of electron donors and sulfate.
- CuxS precipitates were found on non-tyndallized acetate:lactate:sulfate amended bentonite copper disc.

GRAPHICAL ABSTRACT

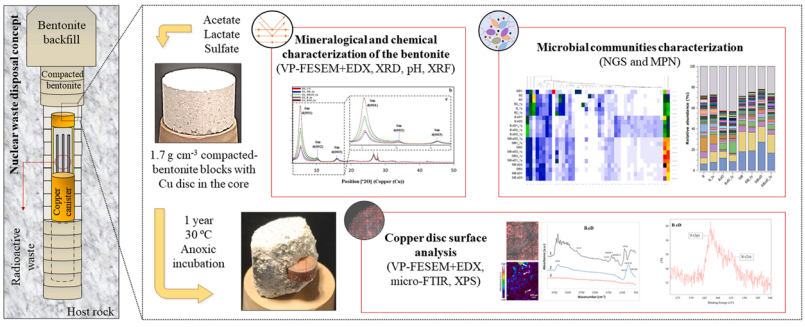

ARTICLE INFO

Editor: Dr. R. Debora

Keywords:
DGR
Compacted bentonite
Microbial diversity
Sulfate-reducing bacteria
Copper corrosion

ABSTRACT

Deep Geological Repository (DGR) is the preferred option for the final disposal of high-level radioactive waste. Microorganisms could affect the safety of the DGR by altering the mineralogical properties of the compacted bentonite or inducing the corrosion of the metal canisters. In this work, the impact of physicochemical parameters (bentonite dry density, heat shock, electron donors/acceptors) on the microbial activity, stability of compacted bentonite and corrosion of copper (Cu) discs was investigated after one-year anoxic incubation at 30 ºC. No-illitization in the bentonite was detected confirming its structural stability over 1 year under the experimental conditions. The microbial diversity analysis based on 16 S rRNA gene Next Generation Sequencing showed slight changes between the treatments with an increase of aerobic bacteria belonging to Micrococcaceae and *Nocardioides* in heat-shock tyndallized bentonites. The survival of sulfate-reducing bacteria (the main source of Cu anoxic corrosion) was demonstrated by the most probable number method. The detection of Cu_xS precipitates on the surface of Cu metal in the bentonite/Cu metal samples amended with acetate/lactate and sulfate, indicated an early stage of Cu corrosion. Overall, the outputs of this study help to better understand the predominant biogeochemical processes at the bentonite/Cu canister interface upon DGR closure.

* Corresponding author.
E-mail address: mmartinezm@ugr.es (M.F. Martinez-Moreno).

https://doi.org/10.1016/j.jhazmat.2023.131940
Received 22 March 2023; Received in revised form 16 June 2023; Accepted 23 June 2023
Available online 26 June 2023

1. Introduction

One of the most relevant issues in the nuclear energy industry is the final disposal and management of high-level radioactive waste (HLW). These waste products generate significant amounts of heat due to the radioactive decay process, whilst also containing large quantities of long-lived radionuclides with a half-life of hundreds to millions of years [4]. For this reason, HLW must be properly and safely confined for at least 100,000 years in suitable facilities until the radiotoxicity decreases to levels comparable to natural ones [60]. The most internationally accepted option for this final disposal is the Deep Geological Repository (DGR), based on a multi-barrier system that isolates the waste from the biosphere. HLW will be stored in corrosion-resistant metal canisters, surrounded by a filling and sealing buffer material (the engineered barriers), and the whole system will be hosted a few hundred meters depth in a stable geological formation (the natural barrier) [87].

The nature of the canisters would depend on the DGR concept adopted by each country. Canada, Korea, and Sweden propose copper as external coating material for metal canisters. Finland has already proceeded to implement Cu as material for metal canisters [65]. Other alternatives include steel-based materials (e.g., Belgium, Czech Republic), titanium (e.g., Japan, United Kingdom), and nickel alloys (e.g., United States of America) [25]. The buffer material in most countries typically consists of highly compacted bentonite clay, which could minimize the groundwater flow, and retard the migration of the radionuclides. Bentonite presents favorable mechanical support providing stability for canisters, low permeability which reduces the groundwater infiltration, high ion exchange that helps with radionuclide retention and retardation in case of containment breach, high plasticity and swelling capacity in order to allow self-sealing of canister cracks, good thermal conductivity, and optimal properties for compaction [20]. In Spain, bentonite from "El Cortijo de Archidona" (Almeria) has been widely studied as a potential buffer material, for DGR use, characterizing its geochemical and mineralogical properties [28,82]. The impact of the microbial community processes in this bentonite, under different relevant DGR conditions, has only began to be studied in the last few years [42,70].

Determination of the structure and composition of the microbial community in the bentonite buffer is crucial to highlight the impact that their activities would have on the long-term stability of the DGR. For instance, microorganisms could affect the integrity of the metal canisters through microbially influenced corrosion (MIC) promoted by biofilm formation on the metal surface or the production of corrosive metabolites. Moreover, in the case of canister cracks or fissures, bacteria could interact with and mobilize radionuclides, increasing their migration through the different barriers. Another implication is related to the microbial metabolism that could contribute to gas phase liberation within the DGR [24]. The main gases produced by microorganisms are in the form of hydrogen (H_2), methane (CH_4), and carbon dioxide (CO_2). These gases would increase the pressure within the DGR, compromising the integrity of the clay barrier [3]. However, certain aspects related to this disposal technology (e.g., compaction density of the buffer material, anoxic conditions, heat produced by the radionuclide waste, etc.) would hinder the activity and viability of the bacterial communities. Upon DGR closure, oxygen will be gradually consumed due to, for example, microbial activity or corrosion of metal canisters (e.g., rock bolts or other steel construction materials), then enhancing an anoxic environment to prevail in the repository [62,33]. Some groups of anaerobic bacteria, such as sulfate-reducing (SRB) and iron-reducing bacteria (IRB), can potentially be active under these conditions. Detrimental effects of the activity of these bacteria include the induction of MIC processes, the reduction of Fe(III) to Fe(II) in the smectite (the main mineral in bentonites), as well as the reduction of sulfate to sulfide (as the main corrosion agent of copper). In addition, some SRB (e.g., *Desulfovibrio vulgaris* and *Desulfitobacterium frappieri*) could cause MIC by reducing the structural Fe(III) in smectite [41,64,74] and producing sulfide, providing sulfate is available in the repository. Sulfide production through reduction of sulfate is kinetically hindered under temperature and pressure standard abiotic conditions [15]. Therefore, the potential presence of sulfide would be originated by the SRB activity [6], which increases at greater distances from the canisters as favorable conditions prevail (e.g., decrease of temperature and increase of water activity). These products could diffuse through the biologically inactive portion of the sealing materials and affect the type and rate of copper corrosion at the container surface. However, diffusion modeling studies suggest that only a small amount of sulfide would actually reach the canisters surface, resulting in a limited impact on container corrosion [35,36,85].

Compaction density of the bentonite is another important issue to be addressed, since the viability and activity of the bacterial communities could be reduced at high dry densities [63]. Nevertheless, microbes are able to survive in a metabolically nearly inactive state or as spores [6,5]. Maanoja et al. [45] reported that the organic matter naturally present in compacted bentonites can sustain biological sulfate reduction by SRB. Accordingly, Povedano-Priego et al. [70] demonstrated the resistance of the microbial communities to high compaction densities (1.5 and 1.7 g cm^{-3}) of the acetate-treated Spanish bentonite, since no significant differences in the bacterial diversity were observed after two years of anaerobic incubation. In addition, SRB groups such as *Pseudomonas*, *Desulfuromonas*, *Desulfosporosinus*, and *Desulfovibrio* were identified. For this reason, the present study is focused on assessing whether the stimulation of microbial activity in highly compacted bentonite (1.7 g cm^{-3}) by the addition of electron donors and acceptors could affect the biogeochemical processes at the bentonite/Cu disc surface interface. Thus, metal-canister corrosion and the mineralogical stability of the clay for long time periods are crucial to be characterized.

Hence, the main aim of the present work was to investigate the biogeochemical and physicochemical processes at the Cu canister/bentonite clay barrier interface-based microcosm and to characterize the biocorrosion products on the metal surface. The studies were focused on assessing the possible one-year-term shifts in the microbial communities of highly-compacted Spanish bentonite containing a copper disc in their core, after one-year anaerobic incubation at 30 ºC. To stimulate the activity of indigenous anaerobic bacteria (e.g., SRB), bentonite was amended with electron donors (acetate and lactate) and an electron acceptor (sulfate), which participate in redox reactions relevant for DGR safety studies [22,49,70]. Microscopic and spectroscopic state-of-the-art techniques were performed to determine the stability of the bentonite and the potential corrosion on the copper disc. Moreover, the most probable number (MPN) technique was carried out to determine viability and quantify the approximate number of SRB per gram in the bentonite samples. Several studies have reported the effect of microbial activity on canister materials or on the stability of commercial bentonites such as MX-80, Opalinus Clay or FEBEX [46,63,75]. Moreover, to the best of our knowledge, this is the first work that collectively describes the impact of indigenous bacteria, from the highly-compacted Spanish bentonite, on the clays' mineralogical stability and the corrosion of copper, whilst also considering the effect of different physiochemical parameters on the bentonite microbial community. Thus, this study lays the baseline to define the microbial effects on both the compacted Spanish bentonite properties, and the initial steps related to long-term corrosion of copper canisters, all of which could affect the safety of nuclear waste storage within the DGR.

2. Material and methods

2.1. Elaboration of compacted bentonite blocks containing a copper disc

2.1.1. Bentonite collection

Bentonite samples were collected aseptically from El Cortijo de Archidona (Almeria, Spain) in February 2020, at a maximum depth of ~ 80 cm. In addition to its safety-related properties, this bentonite has been selected as a reference sealing material for the future Spanish DGR, due to its low carbonate and colloidal contents and a high degree of

plasticity and compressibility [82]. Once in the laboratory, bentonite was stored at 4 ºC until further use.

Bentonites were manually disaggregated and dried under sterile conditions in a laminar flow cabinet for at least 5 days. Then, they were ground with a sterile stainless-steel roller to obtain a homogeneous powder.

2.1.2. Copper disc material

Oxygen-Free High Conductivity (OFHC) copper discs (Cu disc) were obtained from Goodfellow Cambridge Ltd. Company (UNS number C10100; https://www.goodfellow.com). The discs dimensions were 4.0 ± 10% mm of thickness and 10.0 ± 0.5 mm of diameter. The elemental composition was 99.9–100% Cu, with small impurities of S (< 0.0015%), Pb (< 0.0005%), Sb (< 0.0004%), P (< 0.0003%), and Zn (< 0.0001%). Prior to their use, the Cu discs were sterilized by autoclaving 15 min at 121 ºC.

2.1.3. Pre-treatment, compaction process, and incubation conditions

In order to stimulate the microbial activity of anaerobic bacteria (e.g., SRB), the bentonites were sprayed, until a mud-like consistency was obtained, with a sterile mixture solution of sodium acetate (30 mM) and sodium lactate (10 mM) as electron donors. In addition, sodium sulfate (20 mM) was added as a final electron acceptor. Since the addition of electron donors/acceptor in the bentonite does not represent a real DGR scenario, bentonite was amended with the electron donors/acceptor to be able to observe changes in the physico-chemical properties of the clay on a laboratory timescale, as MIC processes would occur too slowly to be observed over the course of our study (1 year incubation). Control samples were only amended with sterile distilled water. The mixture was then dried under sterile conditions in a laminar flow cabinet at room temperature and, afterwards, bentonite samples were ground to a homogeneous fine powder. Additionally, other bentonite series were heat-shocked by tyndallization (110 ºC for 45 min, 3 consecutive days) to reduce the presence and activity of bentonite autochthonous bacteria. A summary of the different treatments is shown in Table 1.

The compaction of the bentonite was conducted in the Laboratorio de Mecánica de Suelos (CIEMAT. Madrid, Spain) following the procedure of Povedano-Priego et al. [70] with some modifications. The amount of bentonite required to compact the blocks to a dry density of 1.7 g cm^{-3} was calculated, taking into account the percentage of the initial moisture, the volume of the cylindrical steel mold (diameter x height: 30.3 × 20.0 mm) and the volume of the copper discs (0.31 cm^3). The initial moisture content (of 12%) was calculated by weighing 2 g from treated bentonite samples before and after desiccation at 110 ºC for 24 h. The procedure (Supplementary Fig. S1) consisted of weighing 13.5 g of dry bentonite, pouring it into the aseptic steel mold, placing the Cu disc in the center of the mold, and then adding another 13.5 g of dry bentonite. Finally, a hydraulic press was used at a pressure of 25–30 MPa to obtain the block.

The compacted bentonite blocks were incubated anaerobically simulating repository-relevant conditions. To provide this anoxic atmosphere, samples were placed into anaerobic jars with anaerobiosis generator sachets (AnaeroGen™, Thermo Scientific), and then incubated at 30 ºC for one year.

Table 1
Nomenclature and summary of the different treatments of bentonite blocks. All samples were compacted to 1.7 g cm^{-3} dry density and contained an OFHC copper disc (Cu disc) in the core.

Sample name	Characteristics	
	Bentonite	Treatment
B.eD	Non-tyndallized	Acetate:Sulfate:Lactate 30:20:10 mM
B	Non-tyndallized	Distilled water
StB.eD	Tyndallized	Acetate:Sulfate:Lactate 30:20:10 mM
StB	Tyndallized	Distilled water

Glossary: **B**: non-tyndallized bentonite, **StB**: tyndallized ('Sterile') bentonite, **eD**: treated with electron Donors and sulfate.

2.2. Topographical, mineralogical, and chemical characterization of compacted bentonite blocks

After one year of incubation, the blocks were taken out from the anaerobic jar. Samples were shattered with the help of a sterilized stainless-steel spatula, and ground to a homogeneous powder with an aseptic mortar, to study the possible changes in the bentonite, as well as in the copper surface. Variable Pressure Field Emission Scanning Electron Microscopy (VP-FESEM) Zeiss SUPRA40VP equipped with an Energy Dispersive X-Ray Microanalysis (EDX) system with a large-area X-Max 50 mm detector was used for the visualization of possible pores or fractures in the compacted bentonite and the analysis of its elemental composition, respectively. The samples were previously prepared for observation by carbon metallization.

Mineralogical characterization and composition of major element analyses were carried out on the homogeneous powder of bentonite by using X-Ray Diffraction (XRD), and X-Ray Fluorescence (XRF), respectively.

XRD was performed using Oriented Aggregates (OA) to study the behavior of the basal reflections of smectite under diverse treatments. Samples were prepared using 0.3 g of bentonite in 3 mL of distilled water [54]. The clay suspension was dispersed by sonication (2 times of 5 min each). Air-dried OA were studied employing a powder X-ray diffraction on a PANalytical X'Pert Pro diffractometer (CuKα radiation, 45 kV, 40 mA) equipped with an X'Celerator solid-state linear detector. A step increment of 0.008º 2Θ and a counting time of 10 s/step were used. Afterwards, the samples were exposed to ethylene-glycol (EG) vapor at 60 ºC for 24 h and re-analyzed with the diffractometer. HighScore software enabled the analysis of the XRD diffractograms.

The bentonite composition in major elements was determined by XRF analysis using PANalytical Zeltium with a rhodium anode ceramic X-ray tube with an ultra-thin high transmission beryllium front window.

The pH of the bentonite samples was measured in triplicate as described in Povedano-Priego et al. [67]. The ground bentonite was mixed and homogenized with 0.01 M $CaCl_2$ in a ratio of 1:15.

2.3. Microbial community study

After one year of anaerobic incubation, the compacted bentonite blocks were stored at − 20 ºC for the total microbial community analysis by culture-independent techniques and at 4 ºC for the culture-dependent techniques. For these analyses, the bentonite blocks were aseptically broken into small fragments, and homogeneously ground with a mortar.

2.3.1. DNA extraction protocol and sequencing

DNA extractions were performed in triplicate for each treatment (B.eD, B, StB.eD, StB). The optimized DNA extraction protocol for compacted bentonites was followed in detail as described in Povedano-Priego et al. [70]. Briefly, 0.3 g of ground bentonite was transferred to 2 mL screw-cap tubes with sterilized glass beads (one of 3 mm diameter and 0.25 g of 0.3 mm diameter). Depending on the samples, a total of 2.4 – 3.6 g of bentonite per replicate was used to reach enough final DNA concentration for sequencing. Subsequently, 400 μL of Na_2HPO_4 (0.12 M pH 8) was added to each tube and vortexed at maximum speed to help DNA desorption from the clay particles. After the extraction, the quantification of the total DNA was performed on a Qubit 3.0 Fluorometer (Life Technology, Invitrogen™).

Amplification, sequencing, and bioinformatics analyses of the extracted DNA were conducted at STAB VIDA (Caparica, Portugal, https://www.stabvida.com). Library construction was performed using the primers 341_F (5′-CCTACGGGNGGCWGCAG-3′) and 785_R (5′-GACTACHVGGGTATCTAATCC-3′) whose molecular target is the V3 – V4 variable region of 16 S rRNA gene [78]. The sequencing was carried

out with Illumina MiSeq platform, using MiSeq Reagent Kit v3 and 300 bp paired-end. After the sequencing, FastQC software was used to perform the quality controls. The generated raw sequence data were analysed using QIIME2 v2021.4 [10]. The reads were denoised using DADA2 plugin in order to trim and truncate low quality regions, dereplicate the reads, and filter chimeras [9]. Rarefaction curves were constructed to determine whether the obtained number of reads reached a reasonable amount. The reads were organized in operational taxonomic units (OTUs) and classified by taxon using the scikit-learn classifier with the SILVA (release 138 QIIME) database (clustering threshold: 99% similarity). The raw data were submitted to the Sequence Read Archive (SRA) at the National Center for Biotechnology Information (NCBI) with the BioProject ID PRJNA947581.

Alpha diversity indices and relative abundance analysis of the annotated OTUs (taxa) were carried out using Explicet 2.10.5 [72]. In order to compare the similarity between samples at genus level, a matric based on Bray-Curtis algorithm were grouped by PCoA (Principal Coordinate Analysis) using Past4 software [26]. Moreover, a heatmap was constructed to visualise OTUs with more than 0.50% of relative abundance. For that, the function 'heatmap.2' and the packages "phyloseq", "gplots" and "RcolorBrewer" were used in R 4.2.1 software [51,57,71,84].

2.3.2. Most probable number of sulfate-reducing bacteria

To determine the effect of acetate, lactate, and sulfate on the microbial community of bentonite, the approximate number of culturable SRB per gram of clay was calculated using the Most Probable Number (MPN) enumeration [27] inoculating the Postgate medium (DSMZ_Medium63, https://www.dsmz.de) and following the MPN Method of Biotechnology Solutions (Houston, USA, https://biotechnologysolutions.com). This technique is based on serial dilutions in triplicate. For this purpose, 1 g of bentonite from each treatment was ground under N_2 atmosphere (mixed from 3 block replicates) and added to 10 mL of a N_2-degassed 0.9% NaCl solution. This mixture was shaken at 180 rpm for 24 h to disaggregate the clay and separate the bacterial cells from the bentonite particles. Afterwards, 1 mL of this suspension was transferred to 9 mL of Postgate Medium in previously N_2-degassed serum bottles until the 10^{-5} dilution. The whole process was carried out in an anaerobic glove box to maintain anoxic conditions. Then, the bottles were sealed and incubated at 30 ºC static and in darkness. After 4 weeks, the presence of black precipitates indicated a positive result. The MPN of SRB was estimated by comparing positive bottles to a reference table (MPN Method, https://biotechnologysolutions.com), taking into account the correction for the initial dilution.

2.4. Copper disc surface analysis

Copper discs extracted from the bentonite blocks were prepared for their observation by VP-FESEM coupled with EDX. The samples were fixed in a 2.5% glutaraldehyde solution in 0.1 M PBS buffer, pH= 7.4 for 24 h at 4 °C. The samples were then washed in the same buffer (3 times for 15 min each at 4 °C) before being post-fixed in 1% osmium tetroxide in darkness for 1 h at room temperature. The samples were washed again in distilled water (3 times for 5 min each), then dehydrated in an increasing concentration gradient of ethanol (from 50% to 100%). Finally, the samples were dried using the Critical Point Drying (CPD) method [2] with carbon dioxide in a Leica EM CPD300 and coated with carbon by evaporation in an EMITECH K975X Carbon Evaporator.

To determine organic compounds, present on the surface of the Cu discs, samples were removed from the bentonites blocks and analyzed with reflectance micro-Fourier Transform Infrared Spectroscopy (micro-FTIR). The samples were not previously prepared or cleaned (unmodified) in order to preserve any potential corrosion compounds or biofilm formation after 1-year incubation. Reflectance micro-FTIR images were obtained using a PerkinElmer Spotlight micro-FTIR spectroscope, equipped with a mercury–cadmium–telluride detector (consisting of 16 gold-wired infrared detector elements). A per-pixel aperture size of 6.25 μm x 6.25 μm was used with two co-added scans per pixel and a spectral resolution of 16 cm^{-1}.

Subsequently, the unmodified copper discs were analysed by X-ray Photoelectron Spectroscopy (XPS). The XPS measurements for surface chemistry were made on a Kratos AXIS Supra Photoelectron Spectrometer. The X-ray source was a monochromated Al Kα source (1486.6 eV), operated with an X-ray emission current of 20 mA and an anode high tension (acceleration voltage) of 15 kV. The take-off angle was fixed at 90° relative to the sample plane. The data were collected from three randomly selected locations and the area corresponding to each acquisition was a rectangle of approximately 110 μm x 110 μm (FOV2 lens). Each analysis consisted of a wide survey scan (pass energy 160 eV, 1.0 eV step size) and high-resolution scan (pass energy 20 eV, 0.1 eV step size) for component speciation. The integral Kratos charge neutralizer was used as an electron source to eliminate differential charging. The binding energy scale was calibrated using the Au $4f_{5/2}$ (83.9 eV), Cu $2p_{3/2}$ (932.7 eV) and $Ag3d_{5/2}$ (368.27 eV) lines of cleaned gold, copper and silver standards from the National Physical Laboratory (NPL), UK. The software CasaXPS 2.3.22 [18] was used to fit the XPS spectra peaks. To compensate for the effect of surface charging, all the binding energies were referenced to the C1s adventitious carbon peak at 285 eV. No additional constraint was applied to the initial binding energy values.

3. Results

3.1. Mineralogical and chemical analysis of the bentonite

After one year of anoxic incubation, the inner Cu disc embedded in the compacted bentonite amended with electron donors (B.eD) was collected, fragmented, and analyzed by VP-FESEM. As shown in Fig. 1, few cracks near the interface Cu disc – compacted bentonite area (Fig. 1**a-b**) and small fissures on the bentonite surface (Fig. 1**c**) were observed. At high magnification, smectite showed the common leaf-like morphology [70] (Fig. 1**d**). These irregularities (fissures and cracks) could be due to the fracturing of the bentonite block.

EDX maps showed the presence and distribution of the elements at the interface compacted bentonite – Cu disc (Supplementary Fig. S2). The major elements in bentonite (Supplementary Fig. S2_a1) were Si, Al, Fe, and Mg (Supplementary Fig. S2_d-g). While no signal of Cu was observed in the bentonite phase, it was entirely detected on the Cu disc (Supplementary Fig. S2 b). Geochemical analyses evidenced no apparent changes among the treatments (Supplementary Table S1). However, the dominant oxides obtained by XRF showed some slight variation after one year of incubation, where SiO_2 indicated a decrease of ~ 3.11%, while Fe_2O_3 and Al_2O exhibited an increase of ~ 1.27% and ~1.16%, respectively. In addition, the values of the pH ranged between 7.7 and 8.2 showing a decrease of ~ 0.42 on average, after one year of incubation (Supplementary Table S1).

The oriented aggregates (OA) technique was performed to identify potential changes in the illite/smectite interstratified clay minerals. XRD patterns of the OA before and after the exposure to ethylene glycol treatment showed no differences between samples (Fig. 2b). Moreover, XRD patterns indicated that smectite (montmorillonite) was the dominant mineral phase, in addition to minority mineral phases such as quartz and plagioclases.

3.2. Effect of the different treatments on microbial communities

3.2.1. Comparison of bacterial diversity after one year of anaerobic incubation

The total DNA from the different treatments, including compacted bentonite blocks prior to the incubation (time 0) and after one year of anaerobic incubation (1 y), was extracted and sequenced in triplicate. Enough sequencing depth was achieved as shown by rarefaction curves (Supplementary Fig. S3), and the Good's coverage index (Table 2). A

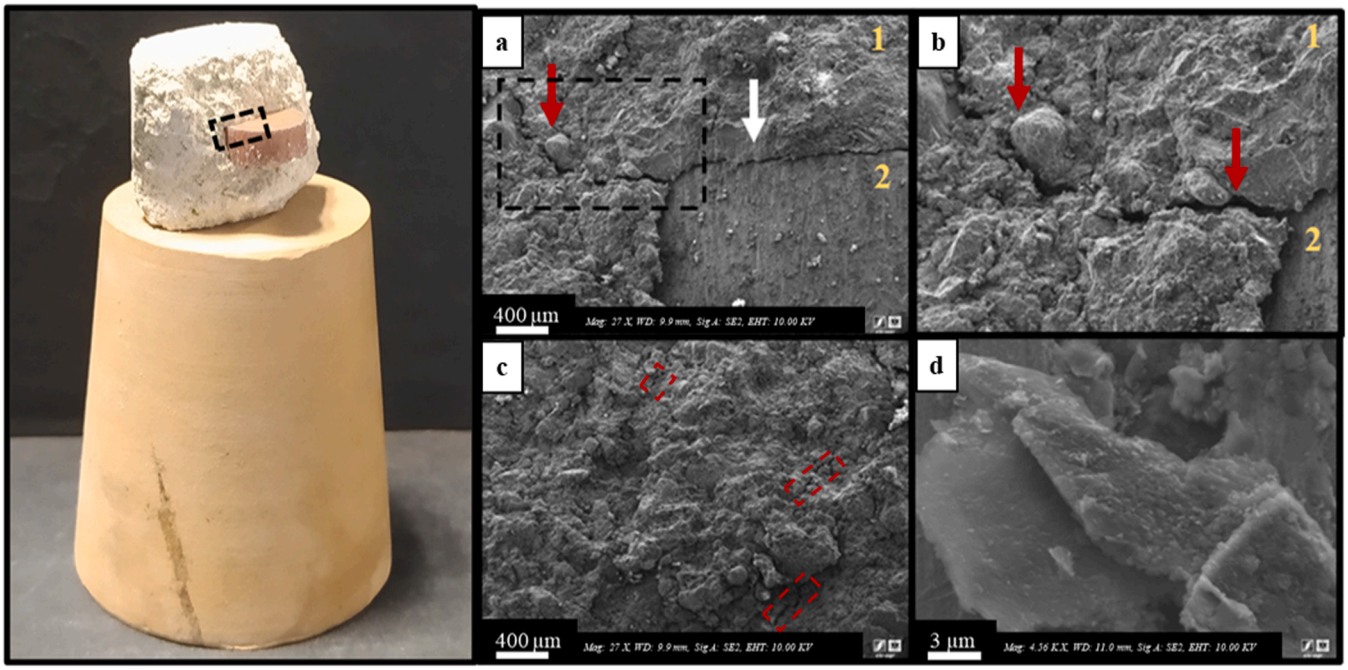

Fig. 1. Left: plowed B.eD bentonite block with copper disc image after one year of anaerobic incubation. (a) SEM images of the selected area in left image, and (b) a magnification of the selected area in (a) showing the topography of the block at the bentonite (1) - copper disc (2) interface (white arrow) and cracks (red arrows). (c) Small fissures in the compacted bentonite (red squares). (d) Leaf-like smectites at high magnification.

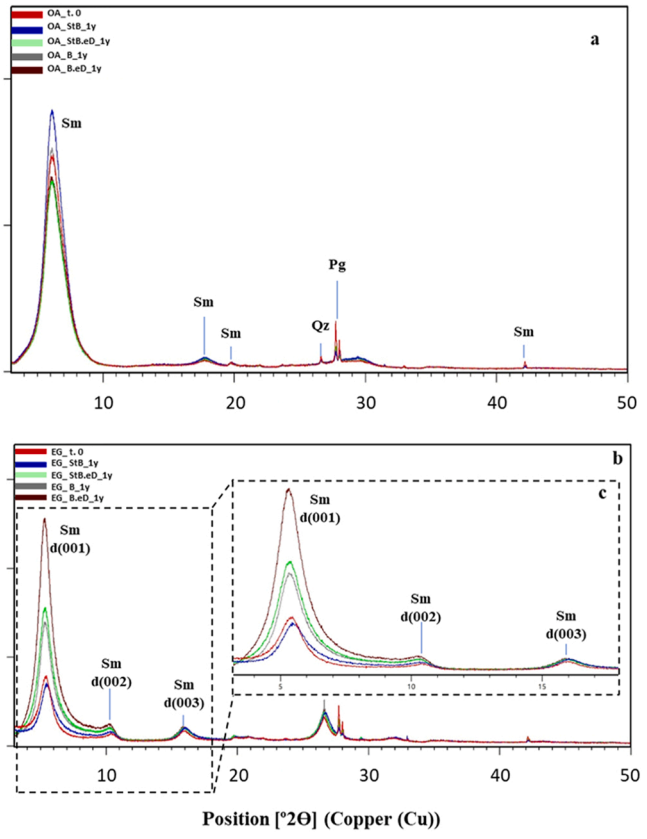

Fig. 2. (a) Oriented aggregates (OA) X-ray diffraction (XRD) patterns of samples t. 0 and after one year of anaerobic incubation (1 y). B: non-tyndallized bentonite blocks, StB: tyndallized bentonite, eD: treated with acetate, sulfate and lactate. Sm: smectite; Qz: quartz; Pg: plagioclase. (b) OA XRD patterns after 24 h at 60 ºC exposure with ethylene glycol (EG) and (c) smectite-illite zone magnification.

Table 2
Good's coverage values, Richness (Sobs), diversity (ShannonH. and SimpsonD), and evenness (ShannonE) indices of the bacterial communities from 1.7 g cm^{-3} compacted bentonite blocks. B: non-tyndallized bentonite, StB: tyndallized bentonite, eD: treated with electron donors and sulfate, 1 y: after one year of anaerobic incubation.

	Good's cov.	Sobs	ShannonH	SimpsonD	ShannonE
B	1.00	437	6.80	0.98	0.78
B_1 y	1.00	471	5.82	0.96	0.65
B.eD	1.00	299	5.62	0.96	0.68
B.eD_1y	1.00	562	6.59	0.97	0.72
StB	1.00	273	4.98	0.92	0.62
StB_1y	1.00	266	5.30	0.92	0.66
StB.eD	1.00	488	5.04	0.89	0.56
StB.eD_1y	1.00	310	5.41	0.93	0.65

range of 63,546 to 431,964 sequence reads was obtained from most samples. Some replicates (i.e.: StB2_1y, B1, and B.eD3) were not included in the analysis due to the low sequencing quality (< 1500).

Richness (Sobs), diversity (ShannonH and SimpsonD), and evenness (ShannonE) indices of the samples are presented in Table 2. An increase in the richness values was observed in the non-tyndallized samples after the incubation period (B_1y and B.eD_1y), while in the tyndallized samples (StB_1y and StB.eD_1y) the value of this parameter decreased. ShannonH and SimpsonD indices indicated a high diversity in all the samples (values > 3 and close to 1, respectively), showing no taxa dominance. However, slightly higher diversity was observed in the non-tyndallized samples, with respect to the tyndallized ones.

A total of 742 OTUs were detected (Supplementary Table S2) and classified in 34 phyla. Of the 34 total phyla, 3 belonged to the Archaea (0.01%), and 31 to the Bacteria domain (99.99%). The Archaea phyla included Aenigmarchaeota in sample B, and Crenarchaeota and Thermoplasmota in sample B.eD, representing ≤ 0.01% within each treatment (Supplementary Table S3). On the other hand, bacterial phyla such as Actinobacteriota (59.48%) and Proteobacteria (24.18%) were the most dominant followed by Chloroflexi (6.05%), Gemmatinomonadota (1.82%), Bacteriroidota (1.77%), and Firmicutes (1.59%). No

remarkable differences were found at phylum level between treatments or incubation times (Fig. 3).

At the genus level, principal coordinate analysis (PCoA), based on the Bray-Curtis distance, showed the dissimilarity of the communities among the different samples (Fig. 4). A clear distinction between tyndallized (StB and StB.eD) and non-tyndallized (B and B.eD) samples was observed. Moreover, non-tyndallized samples were split into two well-differentiated clusters, electron donors/sulfate treated (B.eD), and untreated (B) samples. This last difference between samples B and B.eD (time 0) was potentially due to the fact that after the treatment addition, samples were dried at room temperature for some days until the compaction process was performed, possibly affecting the bacterial growth. This separation was not observed between the tyndallized samples (StB and StB.eD). Additionally, no dissimilarities were found between the samples before and after one year of anaerobic incubation (1y). These results were supported by the heatmap establishing a clear difference between the tyndallized and non-tyndallized samples and, within this last group, between the acetate:lactate:sulfate treated and non-treated samples (Fig. 5).

The microbial communities were mostly represented by *Nocardioides*, unclassified Micrococcaceae, *Promicromonospora* and *Saccharospirilum* (16.32%, 9.77%, 3.97% and 3.93%, respectively). A slight increase (Δ) in the abundance of *Pseudomonas* was observed in B and StB.eD after one year of incubation (Δ 2.98% and Δ 3.04%, respectively) (Fig. 6, Supplementary Table S2). In relation to the heat-shock tyndallization process, unclassified Micrococcaceae and *Nocardioides* were more abundant in the tyndallized samples (StB, StB.eD, StB_1y, and StB.eD_1y) (17.47% and 20.26%, on average) than in the non-tyndallized ones (B, B.eD, B_1y and B.eD_1y) (7.13% and 8.69%, in average), while *Saccharospirillum* and Chloroflexi (Gitt-GS-136) were less abundant after the heat-shock treatment (in average from 5.93% to 0.90%, and from 5.32% to 4.03%, respectively) (Figs. 5 and 6, Supplementary Table S2). Within the non-tyndallized samples, an increase in the presence of Chloroflexi (Gitt-GS-136, and KD4–96), and unclassified Micromonosporaceae was detected in the bentonite amended with electron donors and sulfate. Moreover, some representatives of uncultured Acidimicrobiia, *Sphingomonas*, uncultured Euzebyaceae, *Iamia*, *Vicinamibacteraceae* or *Gaiella* were only detected in the acetate:lactate:sulfate amended treatment within the non-tyndallized samples. In addition, genera such as *Promicromonospora*, *Saccharospirillum*, and *Streptomyces* were slightly more abundant in the unamended treatment within the non-tyndallized samples (Fig. 5 and Fig. 6, Supplementary Table S2).

Regarding bacteria involved in sulfate reduction (SRB), *Desulfosporosinus*, *Desulfotomaculum*, *Desulfuromonas*, *Desulfovibrio*, *Desulfurivibrio*, *Desulfovirga*, and members of the families Desulfurivibrionaceae, Desulfomonadia and Desulfuromonadaceae, among others, were detected in the samples in a very low relative abundance (< 0.2%) (Supplementary Fig. S4 and Table S2). These SRB showed no differences in terms of the addition of acetate:lactate:sulfate after one year of incubation. The most remarkable aspect lays in the enrichment of *Desulfosporosinus* in all the treatments after the incubation (Supplementary Fig. S4 and Table S2).

3.2.2. Viability and most probable number of sulfate-reducing bacteria

The MPN results demonstrated the presence and survival of viable and cultivable SRB in all the treatments (Table 3). The values varied in a range of 2×10^1 and 2.5×10^3 MPN g^{-1} of bentonite (B_1y and B.eD_1y, respectively). This group of microorganisms could be capable of surviving despite the harsh environmental conditions in the bentonite blocks (i.e.: high compaction density and dry environment). Moreover, it was evidenced that SRB are even able to withstand the heat shock produced by the tyndallization process (110 ºC for 45 min, 3 consecutive days) as shown in the StB_1y (1.5×10^3 MPN g^{-1} bentonite), and StB.eD_1y (9.5×10^2 MPN g^{-1} bentonite) samples. In addition, a slight increase in the acetate:lactate:sulfate amended samples after one year of anaerobic incubation (B.eD_1y) was detected (Table 3). A remarkable decrease was observed in sample B (untreated sample) after the incubation time (B_1y). Nonetheless, a slight decrease was detected in the tyndallized amended samples (StB.eD_1y) in comparison to the non-

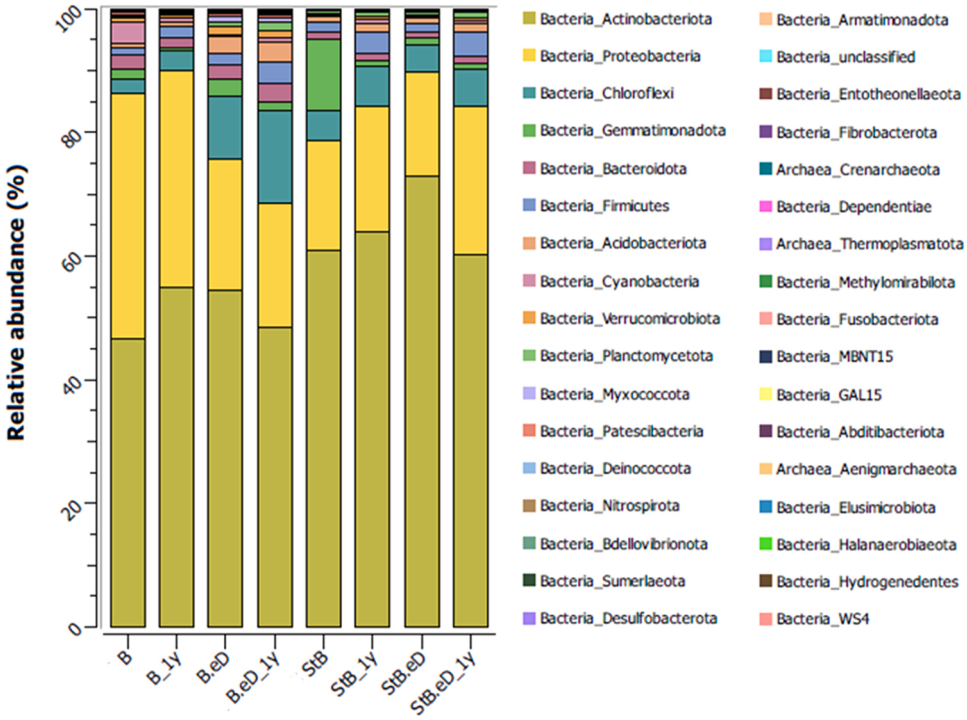

Fig. 3. Phyla relative abundance of the bacterial and archaeal communities from 1.7 g cm^{-3} compacted bentonite blocks. Stacked bars show averages of biological triplicates (duplicates in StB.eD, B and B.eD) B: non-tyndallized bentonite, StB: tyndallized bentonite, eD: treated with electron donors and sulfate, 1 y: after one year of anaerobic incubation.

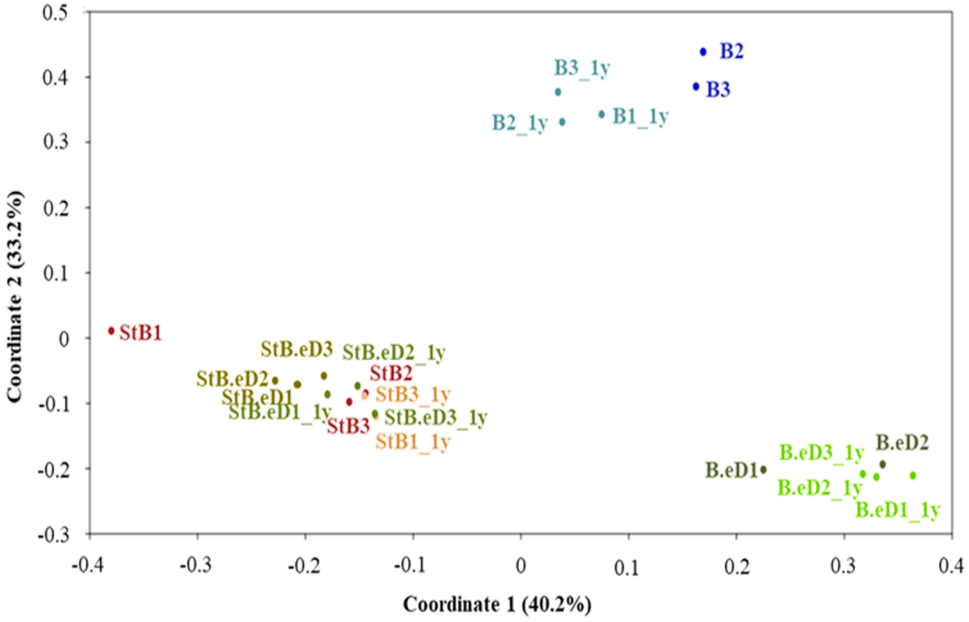

Fig. 4. PCoA (Principal Coordinate Analysis) plot revealing the dissimilarity of microbial genera communities of the 1.7 g cm^{-3} compacted bentonite blocks in triplicate (duplicates in StB.eD, B and B.eD). The distance is based on Bray-Curtis algorithm. B: non-tyndallized bentonite, StB: tyndallized bentonite, eD: treated with electron donors and sulfate, 1 y: after one year of anaerobic incubation.

tyndallized (B.eD_1y) after the incubation period.

3.3. Characterization of the Cu-discs surface

VP-FESEM analyses were carried out on a selection of Cu discs removed from the blocks of each treatment. The data obtained are presented in Fig. 7. Five adjacent areas of ~ 560 × 430 μm were selected from the edge to the center of the disc. The composition of the 5 images from samples B and B.eD showed the distribution of Cu, Fe, Ti, S, Si, Al, O, and C on the surface of the Cu disc (Fig. 7). Micrographs of the discs from tyndallized bentonite and the untreated copper disc (t. 0) indicated no notable changes in the surface of the discs (Supplementary Fig. S5).

The metal surfaces appeared to be practically unaltered. Some damages were observed possibly due to the pressure exerted by some fraction of the bentonite during the bentonite block compaction process. Bentonite traces adhering to the surface of the discs (pink, and blue-green areas) showed Si, Fe, and Al peaks in the EDX spectra (Fig. 7_1 and 7_3). In addition, some yellow-orange areas were possibly related to the presence of small copper oxides confirmed by Cu and O peaks (Fig. 7_2 and 7_4). On the other hand, small blue-almost-white precipitates presented Cu and S peaks may be related to small size copper sulfides (< 1 μm) (Fig. 7_5). An example of unaltered copper zone is shown in Fig. 7_**6**. The presence of carbon in the spectra was related to previous carbon treatment of the samples during their preparation for microscopy analyses.

Reflectance micro-FTIR was used to identify the presence or absence of organic substances on the copper samples. Fig. 8 shows the results obtained from samples B.eD and B (non-tyndallized) with this technique. Areas of the bentonite discs with different treatments were observed using the optical microscope, and then scanned using the infrared microscope. A false-color image is generated showing the locations of infrared-absorbing molecules. An absorbance scale indicates the areas where there is higher abundance of organic or IR-active compounds (red color), or low absorbance regions (dark blue), where usually no IR-absorbing functional groups are present. In all samples, the areas with no IR absorbing molecules presented a relatively flat spectrum, and this is usually superimposed with exposed copper regions in the discs (as seen in the optical microscope). The presence of bentonite was observed on the samples, and when analyzed with micro-FTIR the spectra of these regions usually showed the typical spectra of Si-O, Si-O-Si, AlOH and other inorganic compounds expected on the bentonite-associated regions. Bands related to proteins, lipids and polysaccharides were only detected in sample B.eD, indicating the presence of organic compounds usually associated with the presence of microbial cells or microbial activity in this sample (as shown in Fig. 8). These spectra are very well documented, especially for bacteria related samples [29,56,59,61]. The bands around 3000 cm^{-1} in Spectrum 1 in sample B.eD (Fig. 8) can be attributed to the stretching of oxygen-hydrogen (νO-H). The peaks around 2800 cm^{-1} are normally attributed to methyl (CH_3) and $>CH_2$ functional groups (νC-H). The signals around 1640 and 1540 cm^{-1} corresponded to the amide I and II bands, respectively. The amide I band is due to the stretching carbon-oxygen double bonds (νC═O) within amides associated with proteins and the amide II band is a combination of bending N-H bonds (δN-H) within amides and contributions from stretching C-N (νC-N) groups. The peak around 1400 cm^{-1} is due to the symmetric stretching C-O bond of carboxylate groups (ν_{sym} COO-), while the asymmetric stretching (ν_{asym} COO-) is concealed by the amine II band. The signal around 1760 cm^{-1} corresponds to the vibrational C═O stretching (νC═O) of carboxylic acids. The double bond stretching of phosphate-oxygen >P = O (νP═O), which is connected to phosphodiesters of nucleic acids and general phosphoryl groups, is observed at 1240 cm^{-1}. Tyndallized samples (StB.eD and St.B) showed FTIR spectra similar to sample B where no presence of proteins, lipids or polysaccharides was detected (Supplementary Fig. S6).

XPS analysis was undertaken to assess the surface chemistry of each sample, with wide scans showing the presence of Cu, C, O, Si, Na, P, Fe, Mg and Al on the majority of the samples. The presence of these elements (except for Cu) was likely due to bentonite residues still present on the surface of the discs. The peaks of the Cu $2p_{3/2}$ and Cu $2p_{1/2}$ in the Cu 2p high-resolution scans suggested a combination of elemental copper alongside copper oxide in all samples. As shown in Fig. 9 and Supplementary Fig. S7**,** the Cu $2p_{3/2}$ peaks were observed at 932.4 eV, and the peaks of Cu $2p_{1/2}$ were observed at 952.1 eV, corresponding to elemental Cu and in agreement with tabulated data [83]. However, the presence of peaks likely attributed to CuO were also evident in all samples, as additional peaks were detected around 933.8 eV and 953.5 eV for the Cu $2p_{3/2}$ and Cu $2p_{1/2}$, respectively. No sulfur signal

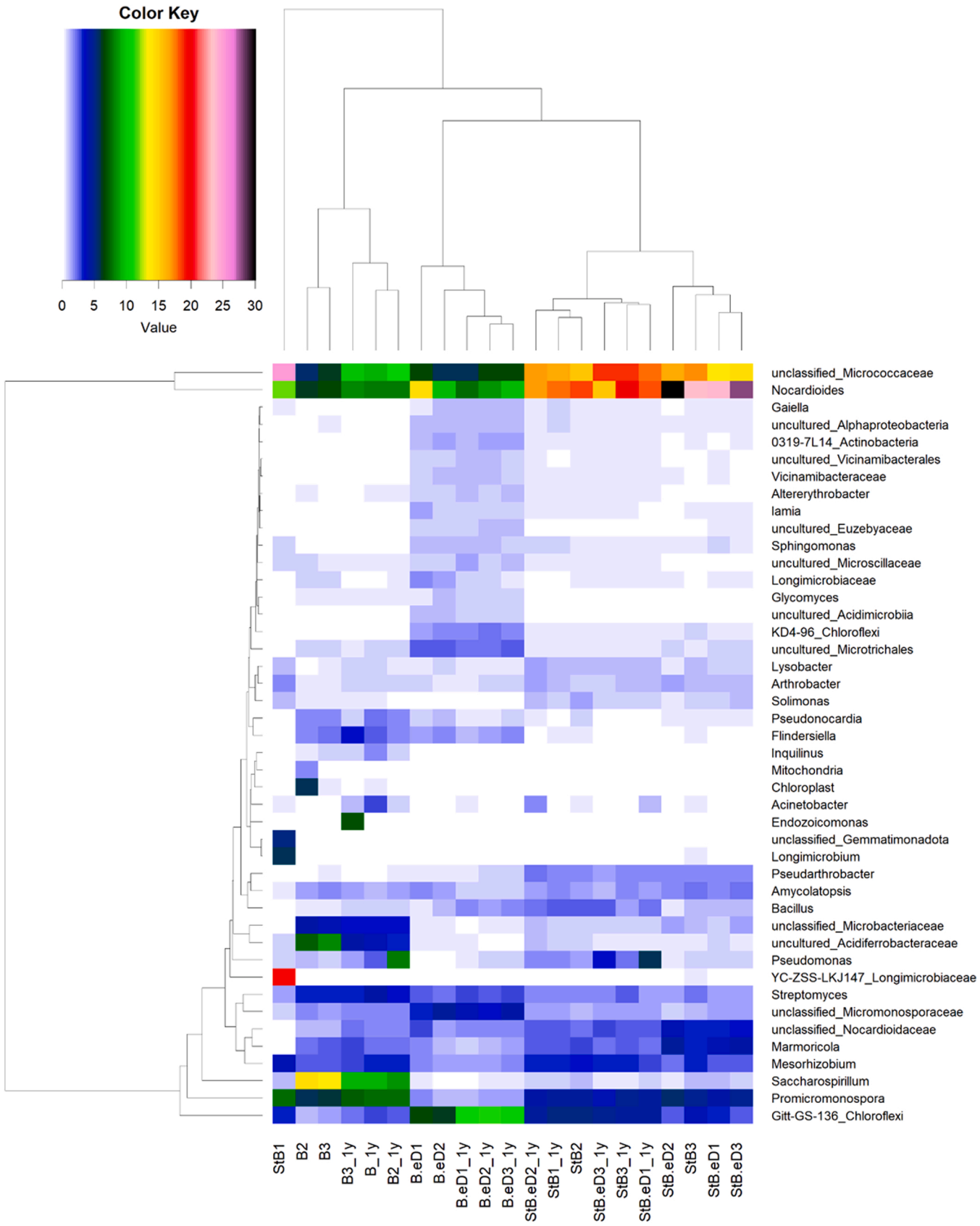

Fig. 5. Heatmap of the relative abundance of the samples at genus level of the 1.7 g cm^{-3} compacted bentonite blocks in triplicate (duplicates in StB.eD, B and B.eD). Cut off: 0.5% of r.a. Different colors show the relative abundance of each genus (the warmer the color, the greater relative abundance). B: non-tyndallized bentonite, StB: tyndallized bentonite, eD: treated with electron donors and sulfate, 1 y: after one year of anaerobic incubation.

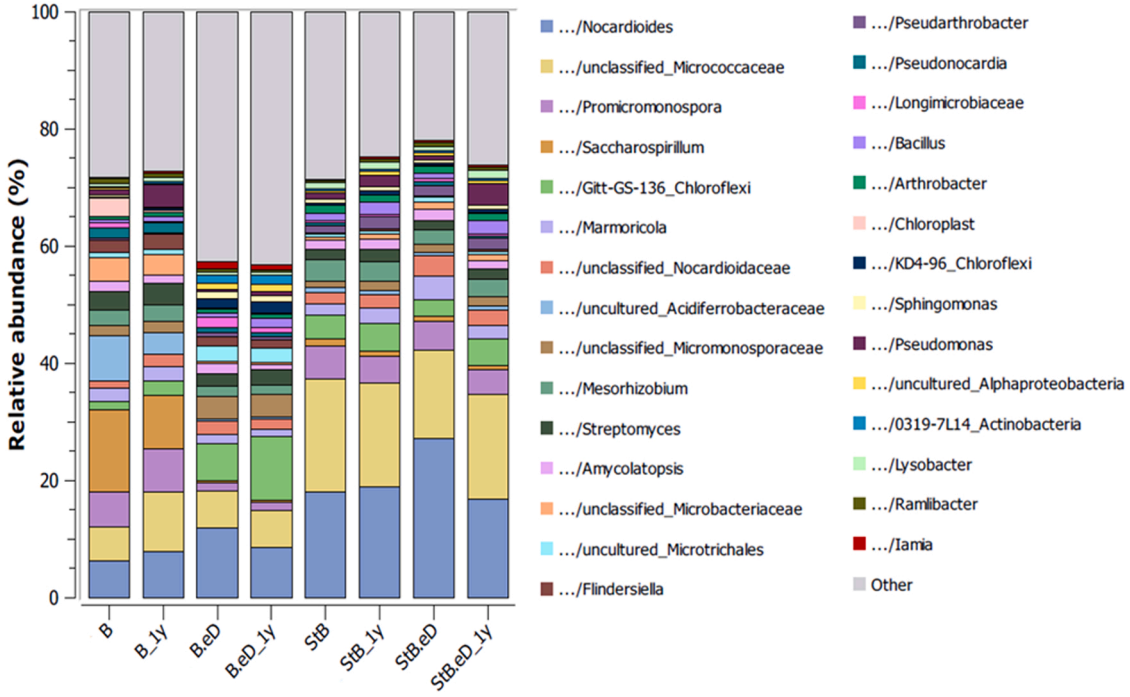

Fig. 6. OTU relative abundance of the bacterial and archaeal communities from 1.7 g cm^{-3} compacted bentonite blocks. Cut-off: 0.6% of relative abundance. Stacked bars show averages of biological triplicates (duplicates in StB.eD, B and B.eD) B: non-tyndallized bentonite, StB: tyndallized bentonite, eD: treated with electron donors and sulfate, 1 y: after one year of anaerobic incubation.

Table 3
Most probable number (MPN) of sulfate-reducing bacteria per gram of three-mixed replicates sample from 1.7 g cm^{-3} compacted bentonite blocks. The value was estimated following the protocol of MPN method from Biotechnology Solutions based in serial dilutions in triplicate in Postgate medium. MPN g^{-1} of bentonite was calculated taking into account the initial pre-dilution to disperse the cells (1 g of bentonite powder in 10 mL of 0.9% NaCl). t. 0: initial bentonite. B: non-tyndallized bentonite, StB: tyndallized bentonite, eD: treated with electron donors and sulfate, 1 y: after one year of anaerobic incubation.

Sample	XYZ pattern*	MPN reading**	3PB dilution***	MPN mL^{-1}	MPN g^{-1} bentonite
t.0	330	25.0	10^0	2.50×10^1	250
B_1y	211	2.00	10^0	2.00×10^0	20
B.eD_1y	330	25.0	10^1	2.50×10^2	2500
StB_1y	210	1.50	10^2	1.50×10^2	1500
StB. eD_1y	320	9.50	10^1	9.50×10^1	950

*XYZ pattern: number of positive bottles after 3PB dilution
* *MPN reading: MNP value from the refence table
* ** 3PB dilution: dilution with 3 positive bottles prior to XYZ pattern

was detected in samples B, StB and St.eD. The peak observed around 155.3 eV in all samples corresponds to Si 2s [13]. In sample B.eD, in addition to the Si 2s signal, a peak at 162.2 eV was observed, indicating the presence of sulfur (Fig. 9).

4. Discussion

4.1. Mineralogical and chemical stability of the bentonite

Although the present work does not focus on an in-depth study of the stability of the physico-chemical properties of bentonite, it is crucial to take into account the impact of microorganisms on the safety-relevant properties of the clay. Meleshyn [52] described how microbial activity could influence these clay properties including the swelling pressure, specific surface area, cation exchange capacity, anion sorption capacity, porosity, permeability, and fluid pressure or plasticity. Microbial processes that could compromise the clay buffer included reduction and dissolution of clay minerals, formation of biofilm, hydrogen sulfide attack produced by sulfate-reducing bacteria, and microbial gas production.

Bentonite from El Cortijo de Archidona (also called FEBEX, Spanish or "Serrata" clay) has been selected by ENRESA (Spanish national radioactive waste company) as the most suitable backfilling and sealing material for a future DGR in Spain. This clay has been widely studied and characterized since the 90's within the FEBEX project (Full-scale Engineered Barriers Experiment) [28]. The mineralogical composition of the bentonite from El Cortijo de Archidona site was previously described by Lopez-Fernandez et al. [44] and consist of smectites (montmorillonite) as the dominant mineral phase (~ 84%) followed by plagioclase (albite), and quartz (~ 12% and ~ 3%, respectively). In addition, this bentonite has a very low organic carbon content, in the range of 0.12 – 0.03%, comparing with other clays such as Opalinus Clay (~ 0.6%) or Boom Clay (1 – 5%) [55,80]. The chemical composition of the studied bentonite (Supplementary Table S1) is very similar to sample BI-2 site reported by Lopez-Fernandez et al. [42] with a decrease in the content of Fe_2O_3 and an increase in the CaO content. Despite the extensive physicochemical characterization of this bentonite, the impact of microbial processes within the DGR concept is still unknown. Therefore, the necessity to elucidate how microorganisms could alter the different DGR barriers is increasing. In the last years, several studies on the microbial communities present in bentonite from El Cortijo de Archidona have been performed [43,44,42,69,68,70,67].

Povedano-Priego et al. [70] focused on studying the impact dry density of compacted bentonite (1.5 and 1.7 g cm^{-3}), amended with acetate after 2-years anaerobic incubation, has on the stability of this clay mineral. The study showed the presence of several cracks and small fissures and, at high magnification, several pores in the 1.5 g cm^{-3}. In general, it is well documented that the more the compaction density of clay increases, the smaller the size and number of pores is [50,53,81]. In the present study, no pores have been observed, which could retard the water diffusion and, therefore, compromise the growth of bacteria [48].

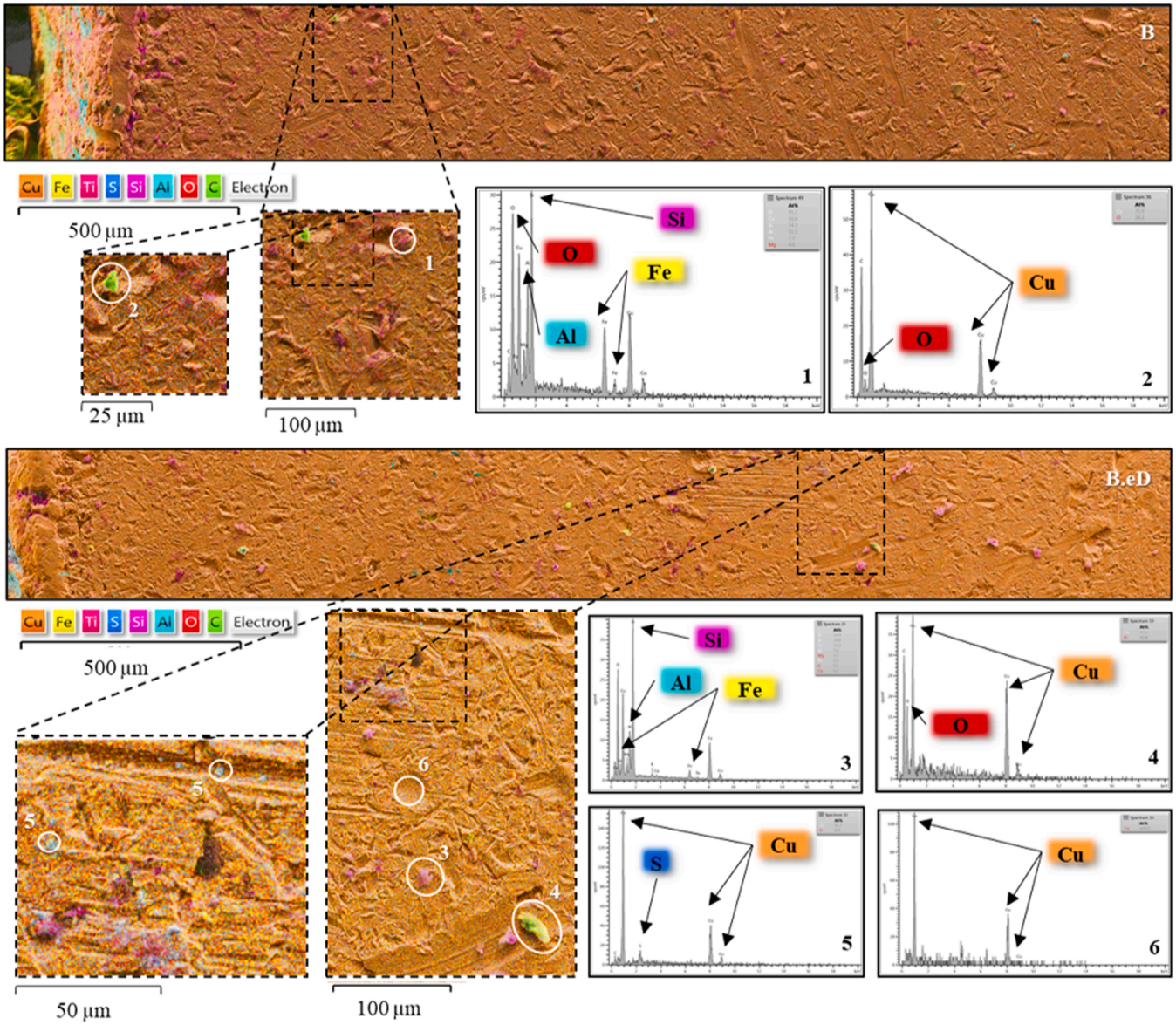

Fig. 7. EDX maps associated with electron images from a selected area (from edge to center) of Cu disc from B and B.eD treatments, respectively. EDX show the distribution of Cu, Fe, Ti, S, Si, Al, O and C in the studied area. White circle and EDX analysis show the presence of bentonite (Si, Al, Fe) adhered to the surface (1 and 3), precipitates related to CuxO (2 and 4), CuxS (5), and unaltered copper (6).

Major elements composition and pH showed no important variations in the bentonite samples, similar to those previously found in uncompacted bentonite samples collected from the same site [44,67]. The stability of bentonite properties is one of the most important issues related to the safety in a DGR [82]. A common concern within the DGR environment is the irreversible smectite-to-illite transformation that would affect the swelling capacity of bentonites [32]. This process depends on many factors such as, for example, high temperatures (100–200 °C) and time. However, some studies have shown that this process can occur at lower temperatures (< 50 °C) [58]. The illitization process may be caused by the attachment of K^+ ions, possibly from the K-feldspars of the bentonite, into the smectite interlayer creating covalent bonds with oxygen. Nonetheless, microorganisms can potentially stimulate this transformation. Microbial metabolism can cause changes in the geochemical conditions of the environment, promoting the smectite-to-illite transformation. The activity of some methanogens and sulfate-reducing bacteria could utilize the structural Fe(III) present in smectite as an electron acceptor coupled with the oxidation of H_2 and/or organic matter, leading to the formation of illite [34]. However, no evidence of illitization process has been observed within our experimental conditions (e.g., effect of the addition of electron donors and acceptor for the stimulation of microorganisms, heat shock, anoxic conditions, etc.) according to the mineralogical and chemical analyses.

4.2. Shifts in bacterial diversity and viability of SRB after one year of anaerobic incubation

Dry and highly compacted bentonite could potentially create a stressful, confined, and starving environment for microorganisms. These conditions could repress microbial activity but not destroy the cells. Therefore, it is important to identify the microbial communities in bentonite and their changes under different DGR relevant conditions. The microbial diversity analyses based on 16 S rRNA Next Generation Sequencing showed slight changes between tyndallized (StB and StB.eD) and non-tyndallized (B and B.eD) samples. Moreover, non-tyndallized samples were split into two well-differentiated clusters, electron donors/sulfate treated (B.eD), and untreated (B) samples. The heat-shock produced by the tyndallization process stimulated an increase of

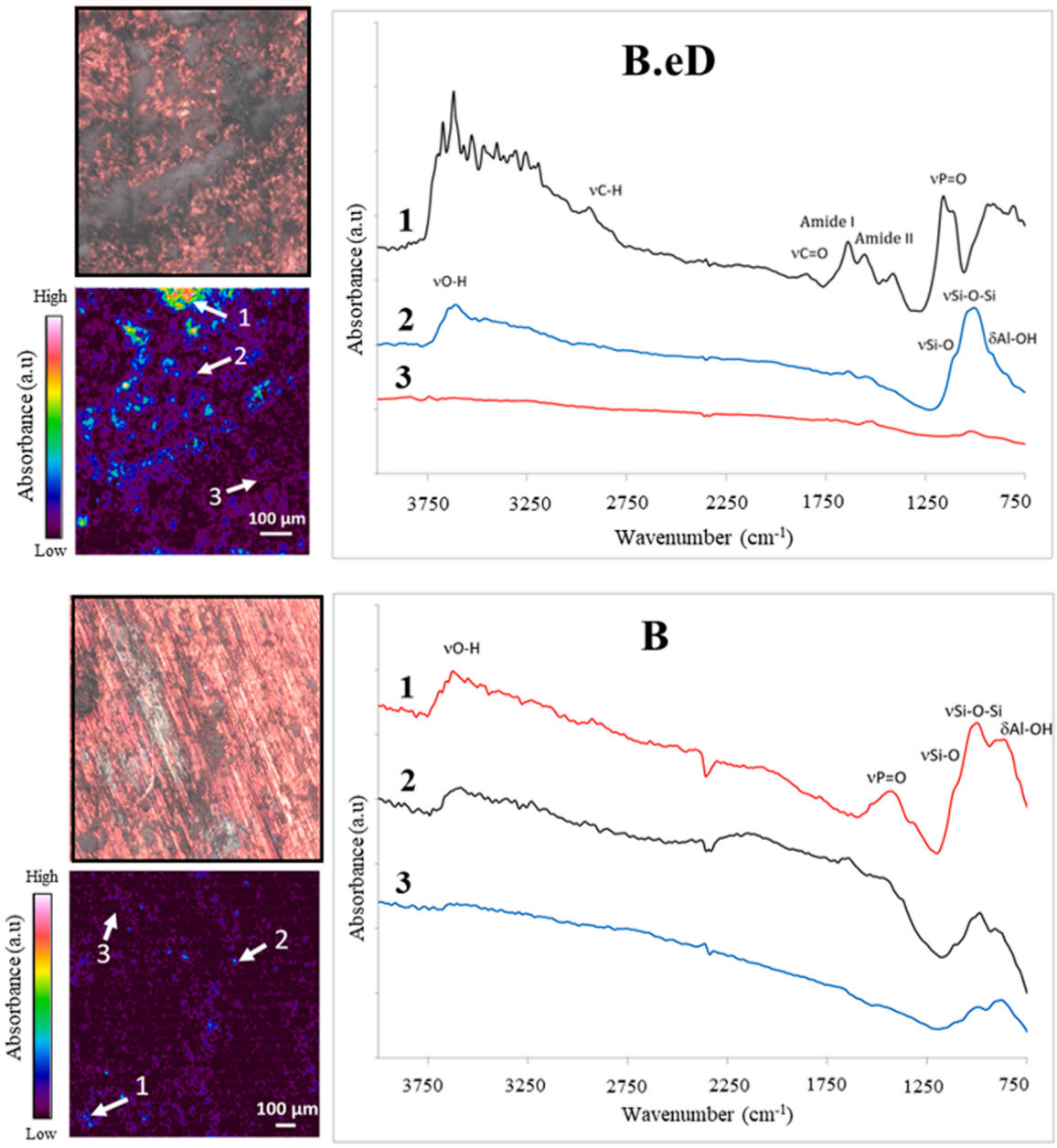

Fig. 8. Reflectance micro-FTIR spectroscopy for the study of microbial presence on the copper disc from sample B.eD and B after 1 year of incubation. Left: optical image of the scanned regions and false-colour image of the sample scanned using reflectance micro-FTIR spectroscopy. Right: infrared spectra of 3 different regions on the samples.

aerobic bacteria belonging to Micrococcaceae and *Nocardioides*. The increase of these aerobic bacteria could be related to the ability of the bentonite to "trap" oxygen molecules that may eventually become available for such bacteria [8]. Additionally, the tyndallization process resulted in non-detectable presence of bacteria such as *Glycomyces* (growth temperature range 15–37 ºC; [39]) or uncultured Acidimicrobiia, while others with growth temperature ranging between 10 and 42 ºC decreased their relative abundance as *Flindersiella*, *Inquilinus, Saccharospirillum* or *Promicromonospora* [12,14,31,88]. This could be explained by the fact that some mesophilic bacteria cannot recover from the exposure to high temperatures, producing thus a pronounceable effect on the bacterial diversity [21]. Despite the potential applications of *Promicromonospora* species, a limited number of reports investigated genomic and phenotypic aspects of these genus members such as multi-resistance to extreme conditions (radiation, desiccation, oxidative stress, etc.) [23]. Therefore, the decrease in relative abundance of the less copious mesophilic bacteria in the samples can cause the more representative ones to increase their presence. An increase in the relative abundance of Chloroflexi members, as well as *Gaiella*, *Sphingomonas*, and *Iamia* has been observed in the acetate:lactate:sulfate amended non-tyndallized samples (B.eD). Although scarce information is available about *Gaiella,* its ability to assimilate acetate and lactate has been reported in *G. occulta* [1]. Similarly, the genus *Sphingomonas* has been proved to assimilate lactate and acetate [79]. Interestingly, some members were able to contribute to the biogeochemical cycle of sulfur through bio-desulfurization (a process for the removal of sulfur from different materials), and in the MIC of copper cold-water pipes [16,86]. On the other hand, it is important for the safety of DGR barriers to consider the presence and activity of SRB, since this bacterial group is the main source of copper corrosion in anoxic conditions through the sulfide production [6]. As shown in this study by metagenomic analyses, several SRB members (e.g., *Desulfosporosinus*, *Desulfotomaculum*, and

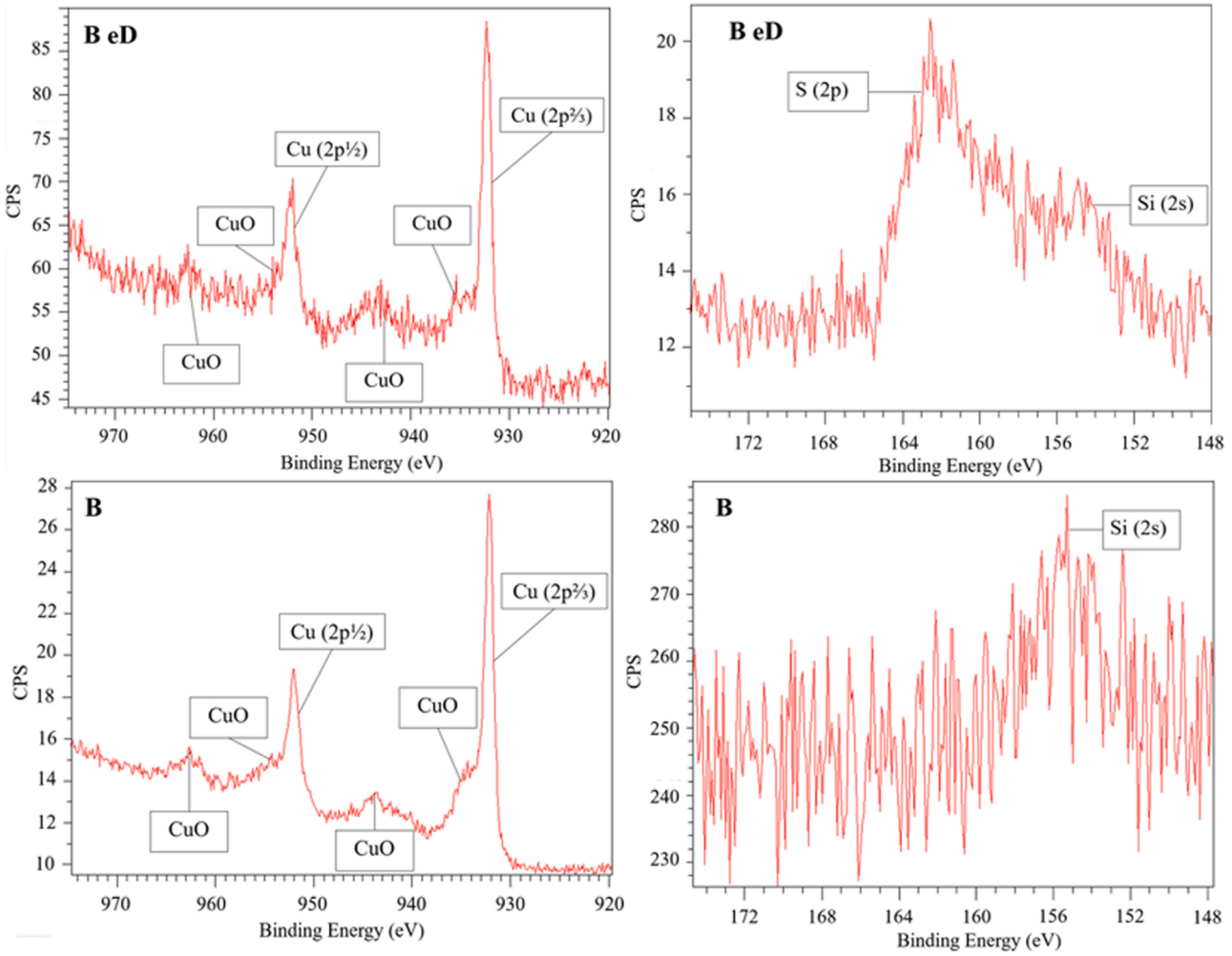

Fig. 9. High resolution XPS scan for the copper 2p region (left), between 975 and 920 eV and for the sulfur 2p region (right), between 175 and 148 eV for sample B. eD (top) and B (bottom) after one year of anaerobic incubation.

Desulfovibrio) have been detected with a very low relative abundance (< 0.2%). According to Povedano-Priego et al. [70], less sequences related to this group were detected in the acetate-amended compacted bentonite. Here, in addition to acetate, lactate and sulfate were incorporated to the compacted blocks, which could have stimulated the growth and detection of more SRB. Additionally, previous studies have shown that species belonging to this group of bacteria were capable of facing these harsh conditions by spore formation in species of *Desulfosporosinus* and *Desulfotomaculum* [22], or by forming desiccated dormant cells in dry bentonite [47]. Therefore, it is worthy to determine the ability of SRB to become active once growth conditions turn favorable (e.g., rewetting and enrichment of organic matter of compacted bentonite through infiltration of groundwater in the repository).

Here by the MPN of SRB, the presence and subsistence of viable and cultivable cells were demonstrated. SRB could be able to withstand the heat shock produced by the tyndallization process as shown in the StB and StB.eD samples. Masurat et al. [47] also observed the resistance of SRB to high temperatures (75 – 120 ºC), showing cell viability after being enriched again in brackish SRB culture medium. In addition, bacterial cells face water loss during desiccation, enhanced by the strong affinity of the bentonite taking the water from the cells leading to cell inactivation and spore formation. The formation of biofilms and sporulation are also well-known strategies used by bacteria to survive desiccation [40]. Yet, the metabolic activity can be restored when water is in contact with the cell again [66]. The compaction at high density (1.7 g cm^{-3}) and the absence of a renewal water flow and/or organic compounds are conditions that make the bentonite blocks a hostile environment for the bacterial growth and viability over time. Previous studies have demonstrated that the increase in the density of the bentonite compaction has a negative effect on the viability of SRB [6, 76]. Nevertheless, it should be noted that the MPN method is only an approximation of the potentially viable SRB cells present per gram of bentonite and the results could depend on several variables, e.g. the samples' storage time at 4 ºC, that could decrease the number of viable anaerobic cells [45]. Thus, these results should be complemented, in future studies, by quantifying specific genes involved in sulfate reduction (e.g., *dsrA* and *aspA*) by qPCR of the bentonite extracted DNA.

4.3. Alteration and corrosion compounds characterization of copper disc

VP-FESEM from sample B.eD and B showed signals related to the presence of the bentonite adhered on the surface of the copper disc (Si, Fe, Al, etc.), supported by XRF analysis (Fig. 7, Supplementary Table S1). The presence of oxygen on the copper surface could be due to the high affinity of copper for oxygen molecules. This oxygen can remain trapped in the bentonite [8] and could participate in the copper oxidation. In sample B.eD, the detection of small precipitates of S associated to copper were detected. This could be related to an initial step of MIC of the copper surface. The increase in the number of SRB found in the MPN experiment may be related to the presence of these precipitates. Under anoxic conditions, SRB are capable of oxidizing lactate (electron donor) coupled to the reduction of sulfate as terminal electron acceptor [77].

The resulting HS^- metabolite could be combined with H^+ to form H_2S. The mechanism of copper corrosion influenced by bacteria is explained elsewhere [17]. Briefly, the H_2S secreted by the SRB can dissociate to H^+ and HS^-. The latter could diffuse to the Cu surface and react with the metal to produce Cu_2S. Several studies have reported copper corrosion mediated by sulfide produced by SRB. Chen et al. [11] showed that, under anaerobic conditions, SRB are able to adhere onto copper surfaces (biofilm) and form a Cu_2S film as the main corrosion product. The production of EPS from the SRB biofilm and, subsequently the Cu_2S film, reduces the toxicity of copper towards SRB. When Cu_2S is removed from the copper surface, the presence of small pits caused by the corrosion effect of SRB could be observed on the material surface. Kurmakova et al. [38] in an experiment with copper and different strains of SRB, showed that these bacteria were responsible for the formation of Cu_2S corrosion products, with *Desulfovibrio* sp. M.4.1 exhibiting the highest corrosive impact on the metal surface. Corrosion of high purity copper in the presence of SRB in groundwater borehole or in MX-80 clay has been demonstrated in other studies where the presence of Cu_2S precipitates have been detected [30,48,63]. Pedersen et al. (2010) in experiments on copper corrosion in compacted bentonite reported the relationship between the sulfur (^{35}S) diffusion coefficient and the compaction density of the clay. This relationship consists of a decrease in the rate of corrosion in the copper material (1.20 m^2 s^{-1} to 0.30 m^2 s^{-1}) as the density increased (1750 Kg m^{-3} to 2000 Kg m^{-3}, respectively) due to, among other factors, the geochemical parameters (e.g., presence of the ferrous iron, capable of immobilizing the sulfide) or the growth conditions of the SRB (e.g., bioavailability of sulfate, electron donors and carbon sources). Accordingly, Johaness et al. (2017) in the post-test examination of three MiniCan test series of copper-cast iron canisters reported similar results. The cast iron showed an integrated corrosion rate of several hundred micrometers per year (μm y^{-1}). Regarding copper, the integrated corrosion rate also decreased as the dry density of MX-80 bentonite clay increased (0.15–0.02 μm y^{-1} in 1300–1600 Kg m^{-3}, respectively).

Micro-FTIR spectroscopy was used to assess the potential presence of microorganisms on the surface of the samples. The occurrence of microorganisms was detected only on sample B.eD. As shown in Fig. 8, the presence of infrared absorption bands corresponding to amides, phosphoryl groups, carboxylic and carboxylate compounds suggested that in this sample the presence of microorganisms could be possible. The distribution of the microorganisms, according to the false-color image in Fig. 8, was not homogeneous or uniform. The IR-absorbing molecules associated with bacteria were localized at discrete locations on the sample, and usually next to areas with spectra that could be attributed to bentonite. Spectrum 2 in B.eD sample (Fig. 8) shows an example of the typical dioctahedral smectite bands from bentonite adhered to the surface of the discs. The band at 3620 cm^{-1} corresponds to the OH stretching for dioctahedral smectites with octahedral sheets rich in Al [89]. Bands related to Si-O and Si-O-Si stretching vibrations bands are detected at 1110 cm^{-1} and 980 cm^{-1}, respectively [19]. The bands around 850 cm^{-1} correspond with bending vibrations of AlOH [7]. Areas showing no IR-absorption bands correspond to the surface of copper only (as can be seen in spectrum 3 in both samples, Fig. 8) and indicate the absence of organic-absorbing molecules above the detection limit of this technique. No evidence of bands related to proteins, lipids or polysaccharides were detected in the samples B, StB and St.BeD (Fig. 8 and Supplementary Fig. S6). In these samples, flat spectra showing no-IR absorbing molecules correspond to the copper surface (dark blue areas in the false-color image), and spectra of bentonite, sulfur-containing compounds (e.g., sulfate) or phosphates; the latter likely to belong to the added electron donors or naturally present in the bentonite.

X-ray photoelectron spectroscopy (XPS) provides a direct chemical characterization of the surface of samples (2–5 nm depth), and has been applied to investigate the composition of the copper discs under the different treatments. In all samples, the presence of elemental copper was evident as shown in Fig. 9 and Supplementary Fig. S7. Sharp peaks were observed at 932.4 eV and 952.1 eV (a separation of 19.7 eV). These peaks have previously been associated with the presence of elemental copper [83], and the binding energies corresponding to Cu $2p_{3/2}$ and Cu $2p_{1/2}$ were observed at 952.1 eV at 932.4 eV, and the peaks of Cu $2p_{3/2}$ peaks Cu $2p_{1/2}$ were observed at 932.1 eV, corresponding to elemental Cu and in agreement with tabulated data [83]. Evidence of anaerobic bio-corrosion on copper surfaces usually involves the presence of Cu_xS compounds. Peaks of CuS in the Cu 2p high resolution region have been previously reported at 932.2 eV for $Cu2p_{3/2}$ [37]. However, as can be seen in Fig. 9, the peaks of elemental Cu in all samples were observed at 932.1 eV, meaning that any potential presence of CuS compounds would have been masked and unable to be detected in these spectra. Therefore, high resolution scans in the region 148–175 eV were performed to assess the presence of sulfur, as this is the region where the S 2p peak would appear if present on the surface of the sample.

High resolution scans in the region between 148 and 175 eV were performed to assess the presence of sulfur and its potential complexation environment. However, no sulfur signal was detected in samples B, StB and St.BeD (Fig. 9 and Supplementary Fig. S7). The peak observed around 155.3 eV in all samples corresponds to Si 2s, previously attributed to silica [13], likely due to bentonite. In sample B.eD, in addition to the Si 2s signal, a peak at 162.2 eV was observed, indicating the presence of sulfur in the form of sulfide. Peaks with binding energy around 162.2 eV have previously been reported as CuS and Cu_2S [37,73]. No peak corresponding to sulfate was detected, as these would have been appeared at binding energies of around 169 eV [37].

The addition of relatively high concentrations of electron donors/acceptor in the bentonite does not represent a real DGR scenario due to the oligotrophic nature of such subsurface environment. However, these nutrients would be able to stimulate the activity of indigenous SRB mainly responsible of the metal surface corrosion on a laboratory timescale, helping to better understand this process in case of enrichment of the bacteria present in the bentonite. The main source of copper corrosion under DGR relevant conditions will be related to the production of hydrogen sulfide. The potential presence of this compound would be originated by the SRB activity [6]. In this study, combining the observations from VP-FESEM, the reflectance micro-FTIR data and the results from XPS, the sample B.eD showed both Cu_xS compounds and the presence of organic compounds, probably of microbial cell origin, on its surface. The infrared spectra of microorganisms were usually in proximity with the bentonite, which could suggest these bacteria could be associated to the bentonite and not directly on the copper surface. The evidence of sulfide-associated compounds also suggests microbial activity of SRB, which could potentially affect the copper surface; however, further tests are needed to verify this hypothesis.

The results presented here shed light for the first time on the microbial activity, bentonite stability, and corrosion of Cu canisters under repository-relevant conditions (e.g., high-density compaction of bentonite, anoxic conditions). This study showed that the mineralogical stability of bentonite was not affected by biotic or abiotic factors. The presence and viability of SRB in all the bentonite blocks, regardless of the treatment, demonstrated the capacity of this bacterial group to survive once the conditions become favorable (i.e., water infiltration). The observed presence of Cu_xS species in the electron donor/sulfate-amended sample (B.eD_1y) could suggest the presence of an early stage corrosion on the copper surface. This study also highlighted the need for further investigation into the bentonite porosity, in order to assess the possible presence of bacterial cells within the pores. In addition, the use of molecular biology techniques, such as qPCR, could provide insights into the activity of SRB by the quantification of the genes involved in sulfate reduction.

5. Conclusions

The present study describes the impact of physicochemical parameters (dry density of bentonite, heat shock, electron donors, and sulfates) on the microbial activity, bentonite stability, and the corrosion of Cu canisters within the concept of DGR. Based on the results of this work, no illitization of smectite was observed in compacted bentonite throughout a year of anoxic incubation at 30 ºC regardless of the treatment. Thus, the stability of bentonite was not affected by biotic (microorganisms), nor abiotic factors (addition of acetate:lactate:sulfate or heat-shock tyndallization process) along the incubation time. Regarding the presence of fractures/pores in the blocks in our study, since this was merely observational, complementary techniques such as mercury intrusion porosimetry test (MIP), atomic force microscopy or permeability studies would be necessary to determine and quantify the porosity of the samples. The addition of acetate, lactate, and sulfate solutions seem to stimulate certain bacterial groups capable of introducing these compounds into their metabolism. In addition, the heat-shock produced by the tyndallization of bentonite seems to slightly shape the bacterial diversity with the enrichment of aerobic bacteria belonging to Micrococcaceae and *Nocardioides*. It is worth noting the presence and viability of SRB in all the bentonite blocks regardless of the treatment. This demonstrated the capacity of this bacterial group to survive despite the harsh conditions in the compacted bentonite and turn functional once the conditions become favorable. SRB are of special importance upon DGR closure since they are the main source of anoxic corrosion of metal canisters. The observed presence of small amounts of Cu_xS species in the non-tyndallized electron donor/sulfate (B.eD) sample could suggest the presence of an early stage of corrosion on the copper surface. The detection of Cu_xS species in the non-tyndallized electron donor/sulfate (B.eD) sample shown minor indication of the corrosion process, as expected given the conditions of the experiment (addition of electron donors and sulfate). In addition, the study aims to understand the long-term behavior of copper corrosion related to DGR, so early detection of corrosion is valuable information for understanding this mechanism in the long term.

Altogether, the results obtained provide new insights in understanding the predominant biogeochemical processes at the bentonite/Cu canister interface upon repository gallery closure.

Environmental Implication

Ensuring the long-term stability of the barriers (e.g., copper canisters and bentonite buffer) of Deep Geological Repository (DGR) is vital to prevent the migration of radionuclides from waste to the biosphere. The present study is pioneering in describing the impact of compacted bentonite microbial communities in the biogeochemical processes at the bentonite/Cu canister interface under DGR relevant conditions. This work showed that, over one-year incubation, no illitization of bentonite and no outstanding copper corrosion are observed. This suggests the mineralogical stability of the Spanish bentonite and the low alteration of copper could have positive implications for future DGRs' long-term safety.

Funding

The present work was supported by the grant RTI2018–101548-B-I00 "ERDF A way of making Europe" to MLM from the "Ministerio de Ciencia, Innovación y Universidades" (Spanish Government). ADM acknowledges funding from the UK Engineering and Physical Sciences Research Council (EPSRC) DTP scholarship (project reference: 2748843).

CRediT authorship contribution statement

Marcos F. Martinez-Moreno: Conceptualization, Methodology, Validation, Investigation, Formal analysis, Visualization, Writing – original draft, Writing – review & editing. Cristina Povedano-Priego: Methodology, Validation, Investigation, Formal analysis, Visualization, Writing – review & editing. Mar Morales-Hidalgo: Writing – review & editing. Adam Mumford: Validation, Formal analysis, Investigation, Writing – original draft, Writing – review & editing. Fadwa Jroundi: Methodology, Formal Analysis, Writing – review & editing. Jesus Ojeda: Validation, Formal analysis, Investigation, Writing – original draft, Writing – review & editing. Mohamed L. Merroun: Conceptualization, Methodology, Formal analysis, Resources, Writing – original draft, Writing – review & editing, Supervision, Project administration, Funding acquisition.

Declaration of Competing Interest

The authors declare that they have no known competing financial interest or personal relationships that could have appeared to influence the work reported in this paper.

Data availability

The raw data were submitted to the Sequence Read Archive (SRA) at the National Center for Biotechnology Information (NCBI) with the BioProject ID PRJNA947581.

Acknowledgements

The authors acknowledge the assistance of Dr. F. Javier Huertas (IACT, Spain) for his guidance and help in collecting the bentonite from the deposit of Almería. Dr. María Victoria-Villar group (CIEMAT, Spain) for the facilities and help during the elaboration of the compacted blocks. Prof. Antonio Sánchez-Navas (Department of Mineralogy and Petrology, University of Garanada, Spain) for his help and training on the diffractometer. Moreover, Concepción Hernández-Castillo and Dr. Isabel Guerra-Tschuschke (Centro de Instrumentación Cientifica, University of Granada, Spain) for the sample preparation and microscopy assistance, respectively. Funding for open access charge: Universidad de Granada / CBUA.

Appendix A. Supporting information

Supplementary data associated with this article can be found in the online version at doi:10.1016/j.jhazmat.2023.131940.

References

[1] Albuquerque, L., França, L., Rainey, F.A., Schumann, P., Nobre, M.F., da Costa, M. S., 2011. *Gaiella occulta* gen. nov., sp. nov., a novel representative of a deep branching phylogenetic lineage within the class Actinobacteria and proposal of Gaiellaceae fam. nov. and Gaiellales ord. nov. Syst Appl Microbiol 34, 595–599. https://doi.org/10.1016/j.syapm.2011.07.001.

[2] Anderson, T.F., 1951. Techniques for the preservaation of three-dimensional structure in preparing specimens for the electron microscope. Trans N Y Acad Sci 13, 130–134. https://doi.org/10.1111/j.2164-0947.1951.tb01007.x.

[3] Bagnoud, A., de Bruijn, I., Andersson, A.F., Diomidis, N., Leupin, O.X., Schwyn, B., Bernier-Latmani, R. 2016. A minimalistic microbial food web in an excavated deep subsurface clay rock. FEMS Microbiol. Ecol. 92:fiv138. https://doi.org/10.1093/femsec/fiv138.

[4] Batandjieva, B., Delcheva, T., Duhovnik, B. 2009. Classification of radioactive waste: safety guide: IAEA General Safety Guide GSG-1. Vienna. International Atomic Energy Agency.

[5] Bengtsson, A., Pedersen, K., 2016. Microbial sulphate-reducing activity over load pressure and density in water saturated Boom Clay. Appl Clay Sci 132, 542–551. https://doi.org/10.1016/j.clay.2016.08.002.

[6] Bengtsson, A., Pedersen, K., 2017. Microbial sulphide-producing activity in water saturated Wyoming MX-80, Asha and Calcigel bentonites at wet densities from 1500 to 2000 kg m^{-3}. Appl Clay Sci 137, 203–212. https://doi.org/10.1016/j.clay.2016.12.024.

[7] Bishop, J., Madejová, J., Komadel, P., Fröschl, H., 2002. The influence of structural Fe, Al and Mg on the infrared OH bands in spectra of dioctahedral smectites. Clay Min 37 (4), 607–616. https://doi.org/10.1180/0009855023740063.

[8] Burzan, N., Lima, R.M., Frutschi, M., Janowczyk, A., Reddy, B., Rance, A., Diomidis, N., Bernier-Latmani, R., 2022. Growth and persistence of an aerobic microbial community in wyoming bentonite MX-80 despite anoxic in situ conditions. Front Microbiol 13, 858324 https://doi.org/10.3389%2Ffmicb.2022.858324.

[9] Callahan, B.J., McMurdie, P.J., Rosen, M.J., Han, A.W., Johnson, A.J.A., Holmes, S. P., 2016. DADA2: high-resolution sample inference from Illumina amplicon data. Nat Methods 13, 581–583. https://doi.org/10.1038/nmeth.3869.

[10] Caporaso, J.G., Kuczynski, J., Stombaugh, J., Bittinger, K., Bushman, F.D., Costello, E.K., Fierer, N., Gonzalez Peña, A., Goodrich, J.K., Gordon, J.I., Huttley, G.A., Kelley, S.T., Knights, D., Koening, J.E., Ley, R.E., Lozupone, C.A., McDonald, D., Muegge, B.D., Pirrung, M., Reeder, J., Sevinsky, J.R., Turnbaugh, P. J., Walters, W.A., Widmann, J., Yatsuneko, T., Zaneveld, J., Knight, R., 2010. QIIME allows analysis of high-throughput community sequencing data. Nat Methods 7, 335–336.

[11] Chen, S., Wang, P., Zhang, D., 2014. Corrosion behavior of copper under biofilm of sulfate-reducing bacteria. Corros Sci 87, 407–415. https://doi.org/10.1016/j.corsci.2014.07.001.

[12] Choi, A., Oh, H.M., Cho, J.C., 2011. *Saccharospirillum aestuarii* sp. nov., isolated from tidal flat sediment, and an emended description of the genus *Saccharospirillum*l. nt J Syst Evol Microbiol 61, 487–492. https://doi.org/10.1099/ijs.0.022996-0.

[13] Clarke, T.A., Rizkalla, E.N., 1976. X-ray photoelectron spectroscopy of some silicates. Chem Phys Lett 37, 523–526. https://doi.org/10.1016/0009-2614(76)85029-4.

[14] Coenye, T., Goris, J., Spilker, T., Vandamme, P., LiPuma, J.J., 2002. Characterization of unusual bacteria isolated from respiratory secretions of cystic fibrosis patients and description of *Inquilinus limosus* gen. nov., sp. nov. J Clin Microbiol 40, 2062–2069. https://doi.org/10.1128/JCM.40.6.2062-2069.2002.

[15] Cross, M.M., Manning, D.A., Bottrell, S.H., Worden, R.H., 2004. Thermochemical sulphate reduction (TSR): experimental determination of reaction kinetics and implications of the observed reaction rates for petroleum reservoirs. Org Geochem 35, 393–404. https://doi.org/10.1016/j.orggeochem.2004.01.005.

[16] Cui, X., Zhao, S., Wang, B., 2016. Microbial desulfurization for ground tire rubber by mixed consortium-*Sphingomonas* sp. and *Gordonia* sp. Polym Degrad Stab 128, 165–171. https://doi.org/10.1016/j.polymdegradstab.2016.03.011.

[17] Dou, W., Pu, Y., Han, X., Song, Y., Chen, S., Gu, T., 2020. Corrosion of Cu by a sulfate reducing bacterium in anaerobic vials with different headspace volumes. Bioelectrochemistry 133, 107478. https://doi.org/10.1016/j.bioelechem.2020.107478.

[18] Fairley, N.CasaX.P.S., 2.3.22 ed.; Casa Software Ltd.: 2019.

[19] Gaggiano, R., De Graeve, I., Mol, J.M.C., Verbeken, K., Kestens, L.A.I., Terryn, H., 2013. An infrared spectroscopic study of sodium silicate adsorption on porous anodic alumina. Surf Interface Anal 45, 1098–1104. https://doi.org/10.1002/sia.5230.

[20] García-Romero, E., María Manchado, E., Suárez, M., García-Rivas, J., 2019. Spanish bentonites: a review and new data on their geology, mineralogy, and crystal chemistry. Fortschr Miner 9, 696. https://doi.org/10.3390/min9110696.

[21] Gilmour, K.A., Davie, C.T., Gray, N., 2022. Survival and activity of an indigenous iron-reducing microbial community from MX80 bentonite in high temperature/low water environments with relevance to a proposed method of nuclear waste disposal. Sci Total Environ 814, 152660. https://doi.org/10.1016/j.scitotenv.2021.152660.

[22] Grigoryan, A.A., Jalique, D.R., Medihala, P., Stroes-Gascoyne, S., Wolfaardt, G.M., McKelvie, J., Korber, D.R., 2018. Bacterial diversity and production of sulfide in microcosms containing uncompacted bentonites. Heliyon 4, e00722. https://doi.org/10.1016/j.heliyon.2018.e00722.

[23] Guesmi, S., Nouioui, I., Pujic, P., Dubost, A., Najjari, A., Ghedira, K., Igual, J.M., Cherif, A., Klenk, H., Sghaier, H., Normand, P., 2021. Draft genome sequence of *Promicromonospora panici* sp. nov., a novel ionizing-radiation-resistant actinobacterium isolated from roots of the desert plant *Panicum turgidum*. Extremophiles 25, 25–38. https://doi.org/10.1007/s00792-020-01207-8.

[24] Guo, G., Fall, M., 2021. Advances in modelling of hydro-mechanical processes in gas migration within saturated bentonite: a state-of-art review. Eng Geol 287, 106123. https://doi.org/10.1016/j.enggeo.2021.106123.

[25] Hall, D.S., Behazin, M., Binns, W.J., Keech, P.G., 2021. An evaluation of corrosion processes affecting copper-coated nuclear waste containers in a deep geological repository. Prog Mater Sci 118, 100766. https://doi.org/10.1016/j.pmatsci.2020.100766.

[26] Hammer, O. 2001. PAST: paleontological statistics software package for education and data analysis. Palaeontol. Electron. http://palaeo-electronicaorg.

[27] Haynes, H.M., Pearce, C.I., Boothman, C., Lloyd, J.R., 2018. Response of bentonite microbial communities to stresses relevant to geodisposal of radioactive waste. Chem Geol 501, 58–67. https://doi.org/10.1016/j.chemgeo.2018.10.004.

[28] Huertas, F., Fariña, P., Farias, J., García-Siñeriz, J.L., Villar, M.V., Fernández, A.M., Martin, P.L., Elorza, F.J., Gens, A., Sánchez, M., Lloret, A., Samper, J., Martínez, M.Á., 2021. Full-scale engineered barriers experiment. Update Final Rep 1994–2004.

[29] Jiang, W., Saxena, A., Song, S., Ward, B.B., Beveridge, T.J., Myneni, S.C.B., 2004. Elucidation of functional groups on gram-positive and gram-negative bacterial surfaces using infrared spectroscopy. Langmuir 20, 11433–11442. https://doi.org/10.1021/la049043.

[30] Johansson, A.J., Lilja, C., Sjögren, L., Gordon, A., Hallbeck, L., Johansson, L., 2017. Insights from post-test examination of three packages from the MiniCan test series of coppercast iron canisters for geological disposal of spent nuclear fuel: impact of the presence and density of bentonite clay. Corros Eng Sci Technol 52, 54–60. https://doi.org/10.1080/1478422X.2017.1296224.

[31] Kaewkla, O., Franco, C.M., 2011. Flindersiella endophytica gen. nov., sp. nov., an endophytic actinobacterium isolated from the root of Grey Box, an endemic eucalyptus tree. Int J Syst Evol 61, 2135–2140. https://doi.org/10.1099/ijs.0.026757-0.

[32] Kaufhold, S., Dohrmann, R., 2010. Stability of bentonites in salt solutions: II. Potassium chloride solution - Initial step of illitization? Appl Clay Sci 49, 98–107. https://doi.org/10.1016/j.clay.2010.04.009.

[33] Keech, P.G., Ramamurthy, P., Vo, S., Chen, J., Jacklin, R., Shoesmith, D.W., 2014. Design and development of copper coatings for long term storage of used nuclear fuel. Corros Eng Sci Technol 49, 425–430. https://doi.org/10.1179/1743278214Y.0000000206.

[34] Kim, J., Dong, H., Yang, K., Park, H., Elliott, W.C., Spivack, A., Heuer, V.B., 2019. Naturally occurring, microbially induced smectite-to-illite reaction. Geol Soc Am Bull 47, 535–539.

[35] King, F. 2002. Status of the copper corrosion model for a deep geologic repository. Ontario Power Generation, Nuclear Waste Management Division Report, 06819-REP-01300–10043-R00.

[36] King, F., Kolar, M., Stroes-Gascoyne, S., Maak, P., 2003. Model for the microbiological corrosion of copper containers in a deep geologic repository. MRS Online Proc Libr (OPL) 807, 811.

[37] Krylova, V., Andrulevičius, M. 2009. Optical, XPS and XRD studies of semiconducting copper sulfide layers on a polyamide film. Int. J. Photoenergy. https://doi.org/10.1155/2009/304308.

[38] Kurmakova, I., Kupchyk, O., Bondar, O., Demchenko, N., Vorobyova, V., 2019. Corrosion of copper in a medium of bacteria sulfate reduction proceeding. J Chem Technol Met 54, 416–422.

[39] Labeda, D.P., Kroppenstedt, R.M., 2004. Emended description of the genus *Glycomyces* and description of *Glycomyces algeriensis* sp. nov., *Glycomyces arizonensis* sp. nov. and *Glycomyces lechevalierae* sp. nov. Int J Syst Evol 54, 2343–2346. https://doi.org/10.1099/ijs.0.63089-0.

[40] Laskowska, E., Kuczyńska-Wiśnik, D., 2020. New insight into the mechanisms protecting bacteria during desiccation. Curr Genet 66, 313–318. https://doi.org/10.1007/s00294-019-01036-z.

[41] Liu, D., Dong, H., Bishop, M.E., Zhang, J., Wang, H., Xie, S., Wang, S., Huang, L., Eberl, D.D., 2012. Microbial reduction of structural iron in interstratified illite-smectite minerals by a sulfate-reducing bacterium. Geobiology 10, 150–162. https://doi.org/10.1111/j.1472-4669.2011.00307.x.

[42] Lopez-Fernandez, M., Fernández-Sanfrancisco, O., Moreno-García, A., Martín-Sánchez, I., Sánchez-Castro, I., Merroun, M.L., 2014. Microbial communities in bentonite formations and their interactions with uranium. Appl Geochem 49, 77–86. https://doi.org/10.1016/j.apgeochem.2014.06.022.

[43] Lopez-Fernandez, M., Vilchez-Vargas, R., Jroundi, F., Boon, N., Pieper, D., Merroun, M.L., 2018. Microbial community changes induced by uranyl nitrate in bentonite clay microcosms. Appl Clay Sci 160, 206–216. https://doi.org/10.1016/j.clay.2017.12.034.

[44] Lopez-Fernandez, M., Cherkouk, A., Vílchez-Vargas, R., Jauregui, R., Pieper, D., Boon, N., Sanchez-Castro, I., Merroun, M.L., 2015. Bacterial diversity in bentonites, engineered barrier for deep geological disposal of radioactive wastes. Microb Ecol 70, 922–935. https://doi.org/10.1007/s00248-015-0630-7.

[45] Maanoja, S., Lakaniemi, A.M., Lehtinen, L., Salminen, L., Auvinen, H., Kokko, M., Palmroth, M., Muuri, E., Rintala, J., 2020. Compacted bentonite as a source of substrates for sulfate-reducing microorganisms in a simulated excavation-damaged zone of a spent nuclear fuel repository. Appl Clay Sci 196, 105746. https://doi.org/10.1016/j.clay.2020.105746.

[46] Madina, V., Insausti, M., Azkarate, I., Garmendia, I., Cuñado, M.A., 2005. Corrosion behaviour of container candidate materials for HLW disposal in granite-bentonite media. Afinidad 62 (519), 383–387.

[47] Masurat, P., Eriksson, S., Pedersen, K., 2010. Evidence of indigenous sulphate-reducing bacteria in commercial Wyoming bentonite MX-80. Appl Clay Sci 47, 51–57. https://doi.org/10.1016/j.clay.2008.07.002.

[48] Masurat, P., Eriksson, S., Pedersen, K., 2010. Microbial sulphide production in compacted Wyoming bentonite MX-80 under in situ conditions relevant to a repository for high-level radioactive waste. Appl Clay Sci 47, 58–64. https://doi.org/10.1016/j.clay.2009.01.004.

[49] Matschiavelli, N., Kluge, S., Podlech, C., Standhaft, D., Grathoff, G., Ikeda-Ohno, A., Warr, L.N., Chukharkina, A., Arnold, T., Cherkouk, A., 2019. The year-long development of microorganisms in uncompacted bavarian bentonite slurries at 30 and 60 °C. Environ Sci Technol 2019 (53), 10514–10524. https://doi.org/10.1021/acs.est.9b02670.

[50] Matusewicz, M., Olin, M., 2019. Comparison of microstructural features of three compacted and water-saturated swelling clays: MX-80 bentonite and Na-and Ca-purified bentonite. Clay Min 54, 75–81. https://doi.org/10.1180/clm.2019.1.

[51] McMurdie, P.J., Holmes, S., 2013. Phyloseq: a R package for reproducible interactive analysis and graphics of microbiome census data. PLoS One 8, e61217. https://doi.org/10.1371/journal.pone.0061217.

[52] Meleshyn, A. 2011. Microbial processes relevant for long-term performance of radioactive waste repositories in clays. GRS-291. ISBN 978–3-939355–67-0. Available from: https://www.grs.de/sites/default/files/pdf/GRS-291.pdf.

[53] Meleshyn, A.Y., Zakusin, S.V., Krupskaya, V.V., 2021. Swelling pressure and permeability of compacted bentonite from 10th khutor deposit (Russia. Minerals 11, 742. https://doi.org/10.3390/min11070742.

[54] Moore, D., Reynolds, R. 1989. X-ray Diffraction and the Identification and Analysis of Clay Minerals. Oxford University Press (OUP). p. 332.

[55] Nagra, 2002. Project Opalinus Clay-safety report: demonstration of disposal feasibility for spent fuel, vitrified high-level waste and long-lived intermediate level waste (Entsorgungsnachweis). Nagra Tech Rep NTB 02–05 (Available from). https://inis.iaea.org/collection/NCLCollectionStore/_Public/50/053/50053802.pdf?r=1.
[56] Naumann, D., Helm, D., Labischinski, H., 1991. Microbiological characterizations by FT-IR spectroscopy. Nature 351, 81–82. https://doi.org/10.1038/351081a0.
[57] Neuwirth E. 2022. _RColorBrewer: ColorBrewer Palettes_. R package version 1.1–3, < https://CRAN.R-project.org/package=RColorBrewer >.
[58] Ohazuruike, L., Lee, K.J., 2023. A comprehensive review on clay swelling and illitization of smectite in natural subsurface formations and engineered barrier systems. Nucl Eng Technol Nucl Eng Technol 55, 1495–1506. https://doi.org/10.1016/j.net.2023.01.007.
[59] Ojeda, J.J., Dittrich, M., 2012. Fourier transform infrared spectroscopy for molecular analysis of microbial cells. J Microbiol Methods 187–211. https://doi.org/10.1007/978-1-61779-827-6_8.
[60] Ojovan, M.I., Steinmetz, H.J., 2022. Approaches to disposal of nuclear waste. Energies 15, 7804. https://doi.org/10.3390/en15207804.
[61] Orsini, F., Ami, D., Villa, A.M., Sala, G., Bellotti, M.G., Doglia, S.M., 2000. FT-IR microspectroscopy for microbiological studies. J Microbiol Meth 42, 17. https://doi.org/10.1016/S0167-7012(00)00168-8.
[62] Payer, J.H., Finsterle, S., Apps, J.A., Muller, R.A., 2019. Corrosion performance of engineered barrier system in deep horizontal drillholes. Energies 12, 1491. https://doi.org/10.3390/en12081491.
[63] Pedersen, K., 2010. Analysis of copper corrosion in compacted bentonite clay as a function of clay density and growth conditions for sulfate-reducing bacteria. J Appl Microbiol 108, 1094–1104. https://doi.org/10.1111/j.1365-2672.2009.04629.x.
[64] Pentráková, L., Su, K., Pentrák, M., Stucki, J.W., 2013. A review of microbial redox interactions with structural Fe in clay minerals. Clay Min 48, 543–560. https://doi.org/10.1180/claymin.2013.048.3.10.
[65] POSIVA. Final Disposal. https://www.posiva.fi/en/index/finaldisposal.html (accessed 16 May 2023).
[66] Potts, M., 1994. Desiccation tolerance of prokaryotes. Microbiol Rev 58, 755–805.
[67] Povedano-Priego, C., Jroundi, F., Lopez-Fernandez, M., Sánchez-Castro, I., Martin-Sánchez, I., Huertas, F.J., Merroun, M.L., 2019. Shifts in bentonite bacterial community and mineralogy in response to uranium and glycerol-2-phosphate exposure. Sci Total Environ 692, 219–232. https://doi.org/10.1016/j.scitotenv.2019.07.228.
[68] Povedano-Priego, C., Jroundi, F., Lopez-Fernandez, M., Morales-Hidalgo, M., Martin-Sánchez, I., Huertas, F.J., Dopson, M., Merroun, M.L., 2022. Impact of anoxic conditions, uranium(VI) and organic phosphate substrate on the biogeochemical potential of the indigenous bacterial community of bentonite. Appl Clay Sci 216, 106331. https://doi.org/10.1016/j.clay.2021.106331.
[69] Povedano-Priego, C., Jroundi, F., Solari, P.L., Guerra-Tschuschke, I., del Mar Abad-Ortega, M., Link, A., Vilchez-Vargas, R., Merroun, M.L., 2023. Unlocking the bentonite microbial diversity and its implications in selenium bioreduction and biotransformation: advances in deep geological repositories. J Hazard Mater 445, 130557. https://doi.org/10.1016/j.jhazmat.2022.130557.
[70] Povedano-Priego, C., Jroundi, F., Lopez-Fernandez, M., Shrestha, R., Spanek, R., Martín-Sánchez, I., Villar, M.V., Sevců, A., Dopson, M., Merroun, M.L., 2021. Deciphering indigenous bacteria in compacted bentonite through a novel and efficient DNA extraction method: insights into biogeochemical processes within the deep geological disposal of nuclear waste concept. J Hazard Mater 408, 124600. https://doi.org/10.1016/j.jhazmat.2020.124600.
[71] R Core Team. 2022. R: A language and environment for statistical computing. R Foundation for Statistical Computing, Vienna, Austria. URL https://www.R-project.org/.
[72] Robertson, C.E., Harris, J.K., Wagner, B.D., Granger, D., Browne, K., Tatem, B., Feazel, L.M., Park, K., Pace, N.R., Frank, D.N., 2013. Explicet: graphical user interface software for metadata-driven management, analysis and visualization of microbiome data. Bioinformatics 29, 3100–3101. https://doi.org/10.1093/bioinformatics/btt526.
[73] Scheer, R., Lewerenz, H.J., 1994. Photoemission study of evaporated $CuInS_2$ thin films. II. Electronic surface structure. J Vac Sci Technol A: Vac Surf Films 12, 56–60. https://doi.org/10.1116/1.578858.
[74] Shelobolina, E.S., VanPraagh, C.G., Lovley, D.R., 2003. Use of ferric and ferrous iron containing minerals for respiration by *Desulfitobacterium frappieri*. Geomicrobiol J 20, 143–156. https://doi.org/10.1080/01490450303884.
[75] Smart, N.R., Reddy, B., Rance, A.P., Nixon, D.J., Frutschi, M., Bernier-Latmani, R., Diomidis, N., 2017. The anaerobic corrosion of carbon steel in compacted bentonite exposed to natural Opalinus Clay porewater containing native microbial populations. Corros Eng Sci Technol, 52(sup1) 101–112. https://doi.org/10.1080/1478422X.2017.1315233.
[76] Stroes-Gascoyne, S., Hamon, C.J., Dixon, D.A., Kohle, C.L., Maak, P., 2006. The effects of dry density and porewater salinity on the physical and microbiological characteristics of compacted 100% bentonite. Mater Res Soc Symp Proc Vol. 985. https://doi.org/10.1557/PROC-985-0985-NN13-02.
[77] Thauer, R.K., Stackebrandt, E., Hamilton, W.A., 2007. Energy metabolism and phylogenetic diversity of sulphate-reducing bacteria. Sulphate-reducing Bact 1–38 https://doi:10.1017/cbo9780511541490.002.
[78] Thijs, S., Op De Beeck, M., Beckers, B., Truyens, S., Stevens, V., Van Hamme, J.D., Weyens, N., Vangronsveld, J., 2017. Comparative evaluation of four bacteria-specific primer pairs for 16S rRNA gene surveys. Front Microbiol 8, 494. https://doi.org/10.3389/fmicb.2017.00494.
[79] Vaïtilingom, M., Amato, P., Sancelme, M., Laj, P., Leriche, M., Delort, A.M., 2010. Contribution of microbial activity to carbon chemistry in clouds. Appl Environ Microbiol 76, 23–29. https://doi.org/10.1128/AEM.01127-09.
[80] Van Geet, M., Maes, N., Dierckx, A., 2003. Characteristics of the Boom Clay organic matter, a review. Geological survey of Belgium. Prof Pap 298, 1–23.
[81] Villar, M.V., Gómez-Espina, R., Campos, R., Barrios, I., Gutiérrez, L. 2012. Porosity changes due to hydration of compacted bentonite. Unsaturated Soils: Research and Applications. Volume 1 (pp. 137–144). Springer. https://doi.org/10.1007/978-3-642–31116-1_18.
[82] Villar, M.V., Fernández-Soler, J.M., Delgado Huertas, A., Reyes, E., Linares, J., Jiménez de Cisneros, C., Linares, J., Reyes, E., Delgado, A., Fernandez-Soler, J.M., Astudillo, J., 2006. The study of Spanish clays for their use as sealing materials in nuclear waste repositories: 20 years of progress. J Iber Geol 32, 15–36.
[83] Wagner, C.D., Riggs, W.M., Davis, L.E., Moulder, J.F., Muilenberg, G.E. 1979. Handbook of x-ray photoelectron spectroscopy: a reference book of standard data for use in x-ray photoelectron spectroscopy. Perkin-Elmer Corporation: Eden Prairie, MN.
[84] Warnes G., Bolker B., Bonebakker L., Gentleman R., Huber W., Liaw A., Lumley T., Maechler M., Magnusson A., Moeller S., Schwartz M., Venables, B. 2022. _gplots: Various R Programming Tools for Plotting Data_. R package version 3.1.3, https://CRAN.R-project.org/package=gplots.
[85] Wersin, P., K. Spahiu, and J. Bruno. 1994. Kinetic modelling of bentonite-canister interaction: Long-term predictions of copper canister corrosion under oxic and anoxic conditions. (No. SKB-TR–94–25). Swedish Nuclear Fuel and Waste Management Co.
[86] White, D.C., Sutton, S.D., Ringelberg, D.B., 1996. The genus *Sphingomonas*: physiology and ecology. Curr Opin Biotechnol 7, 301–306. https://doi.org/10.1016/S0958-1669(96)80034-6.
[87] WNA. World Nuclear Association. 2021. Storage and disposal of radioactive waste. https://www.world-nuclear.org/.
[88] Zheng, W., Li, D., Zhao, J., Liu, C., Zhao, Y., Xiang, W., Wang, X., 2017. Promicromonospora soli sp. nov., a novel actinomycete isolated from soil. Int J Syst Evol Microbiol 67, 3829–3833. https://doi.org/10.1099/ijsem.0.002207.
[89] Zviagina, B.B., McCarty, D.K., Środoń, J., Drits, V.A., 2004. Interpretation of infrared spectra of dioctahedral smectites in the region of OH-stretching vibrations. Clays Clay Min 52, 399–410. https://doi.org/10.1346/CCMN.2004.0520401.